NASA CONTRACTOR REPORT
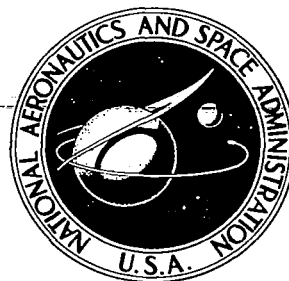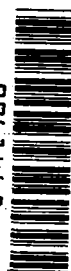
NASA CR-2658

NASA CR-2658

ACCELERATION OF FATIGUE TESTS
FOR BUILT-UP TITANIUM COMPONENTS

R. T. Watanabe

Prepared by
BOEING COMMERCIAL AIRPLANE COMPANY
Seattle, Wash. 98124
for Langley Research Center

NATIONAL AERONAUTICS AND SPACE ADMINISTRATION • WASHINGTON, D. C. • MAY 1976

1. Report No. NASA CR-2658	2. Government Accession No.	3. Recipient's Catalog No.
4. Title and Subtitle ACCELERATION OF FATIGUE TESTS FOR BUILT-UP TITANIUM COMPONENTS		5. Report Date May 1976
		6. Performing Organization Code
7. Author(s) R. T. Watanabe		8. Performing Organization Report No. D6-42768
		10. Work Unit No.
9. Performing Organization Name and Address Boeing Commercial Airplane Company P.O. Box 3707 Seattle, Washington 98124		11. Contract or Grant No. NAS1-12501
		13. Type of Report and Period Covered Contractor Report
12. Sponsoring Agency Name and Address National Aeronautics and Space Administration Washington, D.C. 20546		14. Sponsoring Agency Code

15. Supplementary Notes
Langley technical monitor: Leland A. Imig Final report.

16. Abstract

A study was made of the feasibility of a room-temperature scheme of accelerating fatigue tests for Mach 3 advanced supersonic transport aircraft. The test scheme used equivalent room-temperature cycles calculated for supersonic flight conditions.

Verification tests were conducted using specimens representing titanium wing lower surface structure. Test-acceleration parameters were developed for the test with an auxiliary test set. Five specimens were tested with a flight-by-flight load and temperature spectrum to simulate typical Mach 3 operation. Two additional sets of five specimens were tested at room temperature to evaluate the test-acceleration scheme. The fatigue behavior of the specimens generally correlated well with the proposed correction method.

17. Key Words (Suggested by Author(s)) Fatigue Elevated temperature Ti-6A1-4V titanium Supersonic transports	18. Distribution Statement Unclassified – Unlimited Subject Category 39
19. Security Classif. (of this report) Unclassified	20. Security Classif. (of this page) Unclassified	21. No. of Pages 54	22. Price* $4.25

CONTENTS

CONTENTS (Concluded)

TABLES

FIGURES

FIGURES (Concluded)

ACCELERATION OF FATIGUE TESTS
FOR BUILT-UP TITANIUM COMPONENTS

by R. T. Watanabe
Boeing Commercial Airplane Company

SUMMARY

This report describes an investigation of the feasibility of a fatigue test-acceleration scheme for advanced supersonic transports. The test-acceleration scheme used equivalent room-temperature cycles calculated for supersonic flight conditions.

Verification tests were conducted using specimens representing titanium wing lower surface structure. Test-acceleration parameters were developed for the tests in an "auxiliary" test set of 34 specimens. Five specimens were tested with flight-by-flight loads and cyclic temperature to simulate typical Mach 3 supersonic transport conditions. Two additional sets of five specimens were tested at room temperature to evaluate the test-acceleration scheme.

The fatigue behavior of the specimens correlated well with the proposed elastic correction for the effects of elevated temperature.

INTRODUCTION

Aircraft development programs in the past have proven the value of full-scale tests and such tests will continue to be necessary for future supersonic technology aircraft. It will be desirable to conduct such fatigue tests as rapidly as possible to maximize the time available to resolve deficiencies and to reduce cost. Advanced supersonic transports cruising at Mach 3 will encounter structural temperatures approaching 561 K and will require extensive use of elevated-temperature materials such as Ti-6Al-4V. As much as two-thirds of a probable 50 000-hr design life will be spent at elevated temperature since the high cruise speed will favor long-range flights. During each flight, the structure will be subjected to gust and maneuver induced stresses superimposed on mechanical and thermal stresses such as shown in figure 1. It is therefore apparent that the load and temperature environment for this new generation of aircraft will require more complex fatigue testing considerations than have been customary for subsonic airplanes.

The objective of this investigation is to formulate and demonstrate, by test, a room-temperature test-acceleration procedure for a wing lower surface detail of a Mach 3 supersonic transport. By testing at room temperature, cycling can proceed at rates typical of current tests but analytical techniques must be relied on to a greater degree to account for elevated-temperature effects. The same analytical techniques required for development of equivalent room-temperature test conditions are applicable during design to assess the effects of elevated temperature on fatigue life. These techniques will be valuable in an advanced supersonic transport development program.

SYMBOLS

Physical quantities defined in this report are given in the international system of units (SI, ref. 1). Conversion factors are presented in appendix A to obtain U.S. customary units for SI units used in the present investigation.

E modulus of elasticity, pascals

n number of stress cycles applied, nondimensional

N number of stress cycles to cause failure, nondimensional

R ratio of minimum applied stress to maximum applied stress, nondimensional

S stress, pascals

T temperature, kelvin

t thickness, meters

ϵ axial strain, percent, nondimensional

Subscripts

d design

ET elevated temperature

max maximum

min minimum

RT room temperature

u ultimate

y yield

$1\,g$ load factor corresponding to a vertical acceleration of 1 g

PROPOSED TEST-ACCELERATION METHOD

The basic approach to this test-acceleration scheme is to formulate "equivalent" room-temperature stresses from the projected elevated-temperature operation. This is accomplished by recognizing and accounting for the modifying effects of temperature and applying the equivalent stresses to the structure during a room-temperature test.

The expected operating characteristics of future supersonic transports and the stable behavior of suitable materials under those conditions support the feasibility of this approach. Typically, the ground-air-ground (G-A-G) cycle in each flight (the highest and lowest stresses realized in each flight) contributes at least 75% of the damage per flight. Obviously, emphasis will be placed on this important damage source in a test simulation as it was in the fatigue analysis reported by Doty in reference 2. The G-A-G stresses usually occur early in the flight when airplane mass is relatively large and most of the structure at ambient temperature. The effects of temperature are present, however, and are discussed in the following section.

THERMAL EFFECTS ON SUPERSONIC TECHNOLOGY MATERIALS

The behavior of suitable materials under simulated supersonic transport operating conditions has been the subject of numerous recent investigations. The influence of Mach 3 temperature on fatigue has been shown to be small for titanium alloys and can be evaluated by considering the effects of the following major parameters:

● Thermal exposure

● Fatigue at elevated temperature

● Thermal stress

THERMAL EXPOSURE

No significant change in static properties of suitable materials such as titanium alloys has been observed as a result of long-term exposure to realistic Mach 3 transport stresses and temperatures (ref. 3). The room-temperature fatigue properties of representative structural details, however, frequently suffer a slight reduction after exposure to realistic temperature, i.e., 561 K. Tests by Illg and Imig reported in references 3 and 4 demonstrate this with open hole fatigue specimens exposed continuously to elevated temperature for as much as 3 years. Phillips reported similar results in reference 5 for intermittent temperature exposure on specimens tested outdoors compared with indoor baseline tests. Similar exposure tests of mechanically fastened specimens were conducted by Boeing (ref. 2) in which the exposure degradation was observed to vary with the type of fastener installation. These are shown in figure 2 in terms of cyclic strength reduction at 10^5 cycles. This phenomenon was observed to occur and maximize within 500 hr of exposure to temperatures representative of a Mach 2.7 SST. Most of this thermal effect is probably induced in a shorter time in view of the data reported by Illg and Imig, references 3 and 4.

These investigations generally indicate an absence of creep effects on the fatigue performance of titanium under typical Mach 3 operating conditions. An exception is the unusually long fatigue lives reported in reference 6 for simultaneous real-time peak stress and temperature where the influence of creep mechanisms are suspected. These tests, however, were performed at stresses higher than compatible with long supersonic transport service life requirements and are probably not applicable.

The effect of temperature exposure on supersonic transport structure can be either accounted for by fatigue life reduction factors determined from coupon tests or preferably eliminated as a test variable by exposing the entire test article. Since this exposure condition can be simulated by a short-term single application of heat prior to testing, it could be accomplished by moving a portable bank of heat lamps from section to section on the test airplane.

FATIGUE AT ELEVATED TEMPERATURE

The fatigue behavior of suitable titanium alloys appears to be stable for Mach 3 elevated temperatures. Smith, Hirschberg, and Manson (ref. 7) illustrated the stability of cyclic stress-strain behavior of Ti-6Al-4V by demonstrating that the strain softening experienced at half-life was relatively small. The fatigue performance of unnotched structural materials under moderate elevated temperature can be estimated with the Coffin-Manson equation. Airframe designers, however, are usually faced with complex structure and usually know only the uniform section stresses. Examination of applicable elevated-temperature fatigue test data has indicated that the Coffin-Manson equation can be used on section stress for built-up structure. Thus, equivalent room-temperature stress cycles can be formulated from elevated-temperature cycles based on the elastic modulus variation as shown in figure 3.

Correlations between fatigue strength and modulus of elasticity such as shown in figure 4 (ref. 8) for constant temperature fatigue of notched specimens under fully reversed and tension-tension constant amplitude loads are typical of this technique. Correlation between fatigue life and equivalent stress is shown in figure 5 for notched specimens tested with a programmed load by Imig and Garrett (ref. 6) under room temperature, constant elevated, and varying real-time temperature conditions. These comparisons also demonstrate the importance of the G-A-G cycle in supersonic transport fatigue since they neglect the contributions from gusts and maneuvers. Excellent correlation was obtained with the exception of the one real-time (Type C) case discussed previously. This good correlation of fatigue life with stress supports the use of the equivalent stress method presented in figure 3.

It seems reasonable to expect an upper bound of stress, temperature, or time beyond which the gross-to-peak stress relation will not hold. However, the low stresses required for a long-life commercial transport and the high yield strength of titanium will probably result in essentially elastic structural usage. If so, the preceding correlations would be directly applicable to advanced supersonic transport structure.

THERMAL STRESSES

Thermal stresses encountered during the course of supersonic flight will affect damage accumulation and must be accounted for in a room-temperature simulation. Gust and maneuver induced stress cycles are superimposed on the steady-state stress which consists of mechanical plus thermal stress components. The effect of thermal stress on G-A-G cycles must also be considered since thermal stresses could materially affect the range of the cycle. Tensile thermal stresses are encountered by cold structure and compressive thermal stresses by hot structure as shown in figure 1 for a wing lower surface detail. Thus, the resulting G-A-G cycle differs for different structural elements and the maximum temperature is not necessarily in phase with the maximum combined mechanical and thermal stress. The correlation shown in figure 5 suggests that the fatigue behavior of a structural element under such a general G-A-G cycle could be determined by the equivalent stress method described in figure 3.

TEST PROGRAM

A test program was conducted to demonstrate the feasibility of the proposed acceleration scheme. Two types of test were conducted: auxiliary tests and flight-by-flight fatigue tests (see table 1). Auxiliary tests consisted of static property and constant amplitude fatigue tests to provide parametric data required for the test-acceleration method. The acceleration scheme was then verified by three series of flight-by-flight fatigue tests: a set of baseline tests and two sets of room-temperature simulations.

Test specimens of annealed Ti-6Al-4V were used in the fatigue tests. They consisted of two elements: a skin element and an internal stiffener. The two elements were connected by a row of fasteners to represent a spanwise structural connection (see fig. 6). The hypothetical location of this detail is on the lower surface of a wing. At this location, this structure also encloses a fuel tank, as discussed in a later section.

Most of the auxiliary constant amplitude tests were conducted with specimens consisting of two flat elements (fig. 6a). For flight-by-flight tests, one of the elements was formed into a "hat" section so the specimen could develop thermal stresses and withstand compression loads (fig. 6b). The following paragraphs discuss the results of each group of tests.

Boeing standard "damage" (S-N) curves were used throughout the test program to minimize the number of specimens required. These curves are based on service and test experience and are intended to simulate the behavior of built-up structure under variable amplitude loads. The curves encompass the entire practical range of structural quality (i.e., from unnotched to cracked structure) and fully define life as a function of cyclic stress for each structural quality. Selection of a curve was made by fitting the cyclic stress-life surface through the test data at hand in the life range where fit was desired.

AUXILIARY TESTS

A-1 MATERIAL PROPERTIES

Static material tensile properties were determined for each sheet of material used to fabricate specimens. These data and the corresponding Boeing Material Specifications are shown in table 2.

A-2 ROOM-TEMPERATURE SPECIMEN PERFORMANCE

The room-temperature constant amplitude fatigue behavior of the two types of fatigue specimens is shown in table 3 and in figure 7. The curves shown were fitted through the R = 0.06 test data and expanded to R = -0.35 from the standard constant life relationship. These data show that the forming operation had no significant effect on the fatigue performance of the specimen and that the assumed constant life relationship adequately defines the mean-stress range of interest.

A-3 ELEVATED-TEMPERATURE SPECIMEN PERFORMANCE

The constant amplitude fatigue behavior of the flat specimen at 561 K is shown in table 3 and figure 8. These fatigue data correlated with elastic modulus as shown in figure 9. The present modulus data deviate slightly from the modulus data in reference 9 as shown in figure 9.

A-4 EFFECT OF CYCLIC ELEVATED TEMPERATURE

These tests determined the effect of simultaneous temperature and stress cycling for the flat specimen. Tests with three stress and temperature phase shifts were conducted as shown in figure 10.

Fatigue test data are shown in table 3 and figure 11. The relative fatigue performances for these tests generally supported the correlation with elastic modulus discussed earlier because the lives for cyclic temperatures fell between the life bounds shown in figure 11 for constant temperatures. The lives for the 0° case should have fallen between those for 90° and the constant temperature case as indicated by the example shown in figure 3. The confidence in these data is limited, however, since only three specimens were tested for each phase relation.

A-5 EFFECT OF ELEVATED-TEMPERATURE EXPOSURE

The effect of elevated-temperature exposure on subsequent room-temperature fatigue performance of the flat specimen is shown in table 3 and figure 12. Exposure to 561 K caused approximately 10% reduction in fatigue strength from the unexposed data according to the curve shape used to represent the data.

FLIGHT-BY-FLIGHT FATIGUE TESTS

TEST SPECTRUM

The load spectrum used represented the loading for a wing lower surface detail of a Mach 3 supersonic transport (ref. 10). The loading consisted of basic, 5th, and 100th flights, respectively, applied in a 100-flight sequence. Basic and 5th flights required 60 seconds to apply. The 100th flight required 14 seconds longer because it had more stress cycles.

The 100-flight sequence began with the 100th flight which was followed by four basic flights and 19 sets of one 5th flight and four basic flights. At the end of the last basic flight, the tape was rewound while the specimen was held at taxi conditions. A recording of the programmer basic flight load and skin temperature profile output is shown in figure 13. The 1-g design stress level ($S_{1g,d}$) used for all flight-by-flight tests was 207 MPa.

CUMULATIVE DAMAGE ANALYSIS

A cumulative damage analysis was made to define the fatigue performance for each set prior to conducting the flight-by-flight tests. This also tested the accuracy of the analytical techniques in a design task. The results of this analysis are shown in figure 14. Data generated in the auxiliary tests provided the basic fatigue performance parameters. Standardized room-temperature damage curves matched to specimen fatigue performance were used.

Life fractions (n/N) were calculated with equivalent room-temperature stress cycles for each cycle and its associated temperature. These were computed by dividing the actual stress range by the appropriate modulus degradation ratio for temperature as shown in figure 3. The mean stress for each cycle was the sum of mechanical and thermal stress. The G-A-G cycle was defined as the minimum and maximum equivalent stress in each flight.

The same analysis procedures were employed for the baseline and both accelerated tests. Temperature exposure effects were accounted for in the AC-1 test (see table 1) by factoring the hat specimen damage curve by the fatigue strength degradation ratio observed in the auxiliary tests (A-5).

BASELINE FATIGUE TESTS

The baseline fatigue tests simulated the service conditions of a supersonic transport at the wing location presently considered. These tests included the load spectrum described previously and a temperature cycle for each flight. As described in appendix B, the temperature cycle produced a reversing thermal stress cycle within each flight. The log-average life goal for these tests was approximately 50 000 flights or two equivalent lifetimes. The test stress level was determined from the results of the cumulative damage computations discussed previously. The results of the baseline tests are summarized in table 4 which gives the life, the failure location, and the type of flight at failure.

ACCELERATED FATIGUE TESTS

Test sets AC-1 and AC-2 were used to verify the proposed room-temperature acceleration methods. The AC-1 specimens were exposed to 561 K for 500 hr prior to testing to simulate the effect of long-time temperature exposure on the structure. The AC-2 specimens were tested without exposure. Testing was accomplished at two flights per minute by using only the mechanical load component of the baseline fatigue test.

The fatigue performance was calculated for each set to define the relationship between the accelerated tests and the baseline (BS-1). This was necessary because the same test stresses were used in all flight-by-flight tests and not adjusted to the target (BS-1) life goal of 50 000 flights. As can be seen in figure 14 and table 5, the successful life goals for these two sets were 52 500 flights for the AC-1 and 76 000 flights for the AC-2 test for this simulation. By coincidence, the predicted performance of the AC-1 set was nearly the same as the baseline (BS-1) performance.

TEST RESULT SUMMARY

The results of the flight-by-flight tests shown in figure 15 indicate considerable promise for a room-temperature test simulation. Since these tests were conducted at the same stress level, comparisons must be made with predicted lives.

Test sets BS-1 and AC-1 correlated well with predictions indicating the potential accuracy. Each test was short of predicted life by less than 5%. For the AC-2 tests, the discrepancy was much greater (i.e., the log-average test life was 21% below prediction). The performance of this set was still within reasonable confidence bounds (i.e., 90%), but it is believed that a mechanism related to temperature exposure contributed most of the observed discrepancy since this was the only significant difference between the accelerated sets. A full year separated fabrication and the test during which a low rate degradation could have occurred. The effect of this on the heat soaked set (AC-1) cannot be detected since the elevated-temperature degradation masks any lesser effect.

Additional correlations can be found in the verification tests because of the closed-loop, self-sustaining nature of the test matrix. Each of the constant amplitude auxiliary tests, for example, can be used to provide an excellent representation of the baseline test since the accurate life predictions were made from the auxiliary test data. These simple simulations are not practical for full-scale tests since other damage modifying phenomena such as additional fretting, secondary loads, etc., will be present in a full-scale airframe. Similar tests to verify acceleration techniques must therefore be undertaken on large-scale panels to explore the influence of such secondary effects.

9

CONCLUDING REMARKS

This investigation was conducted to determine the feasibility of accelerating fatigue tests of built-up titanium components. The problem was studied using available data and the proposed scheme verified by fatigue test.

The effect of the expected elevated-temperature environment on titanium structure was found to be small and predictable. Therefore, a test scheme was proposed that employed equivalent room-temperature stresses calculated for the expected temperatures. A single heat soak exposure prior to testing was also suggested.

Verification tests supported the proposed analysis and test-acceleration techniques. Flight-by-flight tests were conducted with specimens representing Ti-6Al-4V wing lower surface structure. Good correlation was obtained between the baseline tests and an accelerated room-temperature simulation having an initial heat soak. Correlation to a lesser degree was obtained for a similar room-temperature case without heat soak indicating the desirability of a heat soak before testing.

APPENDIX A

CONVERSION OF THE INTERNATIONAL SYSTEM OF UNITS TO U.S. CUSTOMARY UNITS

The International System of Units (SI) was adopted by the Eleventh General Conference on Weights and Measures, Paris, October 1960. Conversion factors for the units used herein are from reference 1 and are presented in the following table:

Physical quantity	SI unit	Conversion factor (a)	U.S. customary unit
Frequency	hertz (Hz)	1.0	cps
Force	newtons (N)	0.2248	lbf
Length	meters (m)	39.37	in.
Stress	pascals (Pa)	1.45×10^{-7}	ksi = 1000 lbf/in^2
Temperature	kelvin (K)	$°F = 9/5(K-255.4)$	°F

---

[a]Multiply value given in SI units by conversion factor or apply conversion formula to obtain equivalent value in U.S. customary units.

Prefixes to indicate multiples of SI units are as follows:

Prefix	Multiple
milli (m)	10^{-3}
centi (c)	10^{-2}
kilo (k)	10^{3}
mega (M)	10^{6}
giga (G)	10^{9}

APPENDIX B
TEST PROGRAM DETAILS

MATERIAL

Four 0.91- by 2.44-m sheets each of 1.27- and 2.03-mm-thick Ti-6Al-4V annealed material were obtained specifically for the test program. Each material gage was made from a single heat of material. The chemical composition of the material is given in table 6. Standard tensile specimens having test sections 12.7 mm wide and 50.8 mm long were used to determine the tensile properties of the materials.

FATIGUE SPECIMENS

The two fatigue specimen designs are shown in figure 6. Identical 2.03-mm-thick Ti-6Al-4V annealed skins were used in each type. A 1.27-mm-thick Ti-6Al-4V annealed flat sheet stiffener was used in the flat auxiliary specimen. The stiffener component in the stiffened test specimen consisted of the flat sheet hot-formed into a "hat" section. Mill surface finish was used except that the formed hat section required a slight pickling bath after hot-forming. The longitudinal axis of each element was aligned with the rolling direction of the sheet material.

Eleven titanium fasteners were used in each specimen. The test section consisted of the five central fasteners at which the cross-sectional area was essentially constant. A small amount of skin-to-stiffener load transfer typical of basic structure was induced by selected member planform changes. The stress distributions determined by a simple stress analysis and by a strain gage survey are shown in figures 16 and 17.

FASTENER AND INSTALLATION DATA

The specimen components were fastened with cadmium-plated 4.80-mm-diameter, 100° shear head hex drive Ti-6Al-4V bolts and silver-plated A-286 torque-off collars. They were reworked as follows to preclude embrittlement cracking of the sheet material at elevated temperature. The cadmium was stripped from the bolts by soaking the bolts in a solution of nitric and hydrofluoric acid. The silver plating was stripped from the collars by using nitric acid. After stripping, the bolts were coated with phosphate fluoride and dry film lubricated. The collars were passivated by baking prior to being coated with dry film lubricant. The slight diameter reduction resulting from the stripping process was compensated for in the hole size. Collar torque-off remained within specification.

The fastener diameters after processing were between 4.745 and 4.780 mm. The corresponding hole size used was 4.763 ± 0.013 mm. These were well inside typical production tolerances but were used to minimize test scatter. Final hole size was obtained by reaming matched skin-stiffener pairs using undersize pilot holes as locators. The skin was countersunk in a separate operation to a depth of 1.22 mm or 60% of the 2.03-mm skin thickness. Each step in the fastener installation process was started from a specimen end identified as "upper" and proceeded to the "bottom."

TENSILE TESTS (A-1)

Static properties were determined for each sheet of material using test procedures consistent with ASTM E8-69. An 89-kN capacity electromechanical universal testing machine was used. Load-deflection data were obtained autographically with an X-Y plotter. Elevated-temperature tests were accomplished with an enclosure containing radiant heat lamps. Temperature was regulated to a tolerance of ±3 K during a 1/2-hour presoak and while testing. The test data and applicable Boeing Material Specification (BMS) requirements are shown in table 2.

FATIGUE TEST EQUIPMENT

Standard electronic and hydraulic components and a built-up load frame were used for the fatigue tests. A block diagram of this basic system is shown in figure 18 and the arrangement of the load frame in figure 19. Each specimen had an independent, electrohydraulic, closed-loop servo system capable of applying loads of ±89 kN at frequencies up to 5 Hz. Load accuracy was within ±1% of the full-scale load. Each test specimen was mounted in line with a dual-bridge strain gage load cell as shown in figure 19. The output of one bridge was normally monitored on the load readout console, while the other bridge provided continuous feedback to the servo controller. A strip chart recorder was connected to the load cell to provide load-versus-time recordings when required. Strip chart recorders were also used to obtain load and temperature-versus-time recordings.

Elevated temperature was controlled by existing Boeing-designed temperature and power regulators. Chromel-alumel thermocouples were bonded to the specimens to provide the feedback signal for maintaining accurate specimen temperatures. Quartz lamps mounted on radiant heater assemblies were used to provide the heat required. When required, plant air was used to cool the specimen.

ROOM-TEMPERATURE FATIGUE TESTS (A-2)

The room-temperature fatigue performance (S-N curve) of the two fatigue specimen types (fig. 6) was determined with test set A-2. A static stress survey of one specimen of each type before fatigue testing produced the stress-distributions shown in figures 16 and 17.

Fatigue testing was conducted with constant amplitude sinusoidal loads at a rate of 2 Hz. Load control was provided by Boeing-designed programmers employing motor-driven precision sine potentiometers. For the two static survey specimens, the maximum fatigue loads equaled or exceeded the static load. Failure in all subsequent fatigue tests was defined as a crack reaching a free edge.

ELEVATED-TEMPERATURE FATIGUE TESTS (A-3)

The effect of constant 561 K temperature was determined for the flat specimen with test set A-3. Temperature distribution surveys were run on the first (-9) specimen before fatigue cycling to determine the best heat lamp setup. The objective of the survey was to obtain a uniform temperature distribution at the fasteners in the test section (fasteners 4 through 8). To promote uniform heating, the specimens were completely painted with heat-curing flat black silicone lacquer and shielded in certain areas with an asbestos-type material. The best distribution was obtained with the lamps tilted away from the specimen at the upper ends and the entire assembly surrounded with an enclosure to minimize drafts. This is shown in figure 20. Thirteen temperature surveys were made with temperature at 561 K. A temperature distribution representative of the final setup is shown in figure 21. The finalized heating setup was then duplicated for the other four specimens. Fatigue cycling was conducted at 2 Hz with sine potentiometers.

CYCLIC ELEVATED-TEMPERATURE FATIGUE TESTS (A-4)

The effect of simultaneous temperature and stress cycles was determined in tests of flat specimens. Three stress and temperature phase shifts were investigated as shown in figure 10. Temperature cycled between 328 K and 561 K at 0.0167 Hz. The same profile was also used for the mechanical load to minimize the number of system programmers required. Three matched automatic, curve-following programmers were used to provide a controlled input for constant amplitude heat and load cycling. One programmer was used for temperature control of all specimens and the in-phase load. The other programmers controlled the out-of-phase (90° and 180°) loads. No mechanical coupling was necessary as all programmers had synchronous drum motors and excellent timing was obtained.

Temperature distribution surveys were run on the first (-14) specimen prior to fatigue testing. Some difficulty was experienced in obtaining an acceptable distribution and in attaining desired minimum temperatures. The distribution problem was found to be restricted to the survey specimen and was apparently caused by the thermocouples mounted on it. No satisfactory distribution data were obtained but test runs on the other four available specimens indicated that distributions typical of the A-3 set were obtained. Approximately 20 survey cycles of temperature were applied to the specimen during setup. Load was not applied during the survey.

ELEVATED-TEMPERATURE EXPOSURE (A-5)

The effect of elevated-temperature exposure on the room-temperature fatigue performance was determined for the flat specimen. The specimens were heated in an oven at 561 K for 500 hr. No attempt was made to control environmental parameters other than temperature during exposure. Fatigue testing was conducted at room temperature with sinusoidal constant amplitude loads at a rate of 2 Hz.

FLIGHT-BY-FLIGHT TESTS

The spectrum loads and temperatures required in the flight-by-flight tests were programmed for a multichannel digital programmer using a five-track magnetic tape 12.7 mm wide and 730 m in length. Each data point represented a specific increment of full-scale output of one programmed channel. Load was programmed on one channel, the temperature profiles on two channels, and air on one channel. The fifth channel was used for a temperature check system. The digital data were converted to an analog voltage for the closed-loop servohydraulic and radiant heat systems.

The statistical stress variations for a 100-flight sequence (basic, 5th, and 100th) were included, starting with the 100th flight. The remaining 99 flights consisted of four basic flights and 19 sets of one 5th and four basic flights. Basic and 5th flights required 60 sec to apply but, due to the large number of alternating cycles during climb, the 100th flight required 14 sec longer. Programmer diagrams of the load for a basic flight are shown in figure 13. The 1-g design stress level ($S_{1g,d}$) used for all flight-by-flight tests was 207 MPa.

BASELINE FATIGUE TESTS (BS-1)

The baseline test represented the service experience for a supersonic transport wing lower surface. Five stiffened hat specimens (fig. 6) were tested with a combined spectrum of thermal and mechanical flight-by-flight loads and temperatures. The temperature and thermal stress cycle was based on an assumed 2-hr mission as shown in figure 22. The temperatures shown were determined by finite difference solutions of the Fourier law of heat conduction for a segment structural model of the cross section. Thermal stresses were calculated for a segmented section by analyzing the structure as a beam with freedom to expand without rotation. By assuming the structure to be part of a fuel tank that is emptied at midcruise, fully reversing temperature gradients were included in the cycle. Significant thermal stresses developed early in the flight as a result of the fuel present. With no fuel present during late cruise, the interior absorbed heat, producing an opposite gradient during descent.

Similar analytical techniques were used to formulate the test cycle. Since testing speed was important, heating and cooling were accomplished as rapidly as possible. Therefore, the temperature profile from the A-4 test was used for the skin-stringer material at the fasteners. The stiffener free flange temperature profile was devised to ensure realistic stress and temperature combinations for the material at the fastener row. The resulting profiles are shown in figure 23. The skin temperature profile and the mechanical loads for the basic flight are shown in figure 13. Continuous air cooling was programmed during the early climb segment of the 100th flight (start of the 100-flight sequence) and at the end of the last basic flight while the tape was rewound.

Before fatigue cycling, thermal strain and temperature surveys were made with the programmed temperatures to determine the best lamp and air system configuration. The mechanical load spectrum was not applied during the survey. Instead, a steady load of 31.14 kN was applied to simulate specimen distortion from typical tensile flight

loads. The temperature distribution was obtained by recording thermocouple outputs. The insulation used to separate the thermal behavior of the skin from the stiffener free flange is shown in figure 24. Two temperature cycles (two flights) were completed before recording to avoid transient readings. Each thermocouple (see fig. 25) was read on one of the remaining flights. The planform maximum and minimum temperature distributions are shown in figure 26.

Three thermocouple-strain gage pairs were monitored continuously to provide temperatures and thermal stresses for a representative test flight. The instrumentation output was recorded on a multichannel oscillograph which allowed instantaneous measurements. The strain gage data were corrected for the nonlinearity of free thermal strains, for the strain error caused by the heat protective shield on each gage, and for the changes in the elastic modulus of the specimen material. The resulting data for the sixth flight of the final string of survey flights are shown in figure 27. Thermal stresses for the skin and stiffener flange are shown for a location between fasteners 4 and 5. Stress estimates at the location between fasteners 5 and 6 are also shown. These were necessary because the strain gage was burned out by the large number of heat cycles applied to the specimen during the survey. These estimates were based on the observed relationship between the strain gages during surveys conducted before the final changes in the air cooling system. Confidence in this procedure is high since the thermal stresses obtained for given skin-flange temperature pairs were very stable during the temperature cycles.

ACCELERATED FATIGUE TESTS

Five hat specimens were subjected to 561 K for 500 hr prior to testing. Fatigue tests were then conducted at room temperature with the mechanical load component of the program tape. The loads, however, were applied at twice the rate (two flights per minute) used in the baseline test to ease scheduling requirements.

Five additional stiffened hat specimens were tested (AC-2) to simulate a room-temperature test of test article in the "as manufactured" state. Fatigue loads were the same as for the AC-1 tests.

16

REFERENCES

1. Mechtly, E. A.: *The International System of Units–Physical Constants and Conversion Factors (Second Revision).* NASA SP-7012, 1973.

2. Doty, R. J.: *Fatigue Design Procedure for the American SST Prototype. Advanced Approaches to Fatigue Evaluation.* NASA SP-309, 1972, pp. 365-404.

3. Illg, W.; and Imig, L. A.: *Fatigue of Four Stainless Steels, Four Titanium Alloys and Two Aluminum Alloys Before and After Exposure to Elevated Temperature to Up to Three Years.* NASA TN D-6145, April 1971.

4. Imig, L. A.: *Effect of Initial Loads and of Moderately Elevated Temperature on the Room-Temperature Fatigue Life of Ti-8Al-1Mo-1V Titanium-Alloy Sheet.* NASA TN D-4061, August 1967.

5. Phillips, E. P.: *Effect of Outdoor Exposure at Ambient and Elevated Temperatures on Fatigue Life of Ti-6Al-4V Titanium Alloy Sheet in the Annealed and the Solution-Treated and Aged Condition.* NASA TN D-7540, June 1974.

6. Imig, L. A.; and Garrett, L. E.: *An Investigation of Fatigue Test Acceleration for Conditions of MACH-3 Flight Using Flight-by-Flight Loading.* NASA TN D-7380, 1973.

7. Smith, R. W.; Hirschberg, M. H.; and Manson, S. S.: *Fatigue Behavior of Materials Under Strain Cycling in Low and Intermediate Life Range.* NASA TN D-1574, October 10, 1962.

8. Lockheed-Georgia Co.: *Determination of Design Data for Heat Treated Titanium Alloy Sheet.* ASD-TDR-62-335, vols. 1-3, 1962.

9. *Metallic Materials and Elements for Aerospace Vehicle Structures.* MIL-HDBK-5B, 1974.

10. Imig, L. A.; and Illg, W.: *Fatigue of Notched Ti-8Al-1Mo-1V Titanium Alloy at Room Temperature and 550°F (560°K) With Flight-by-Flight Loading Representative of a Supersonic Transport.* NASA TN D-5294, July 1969.
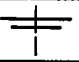
Table 1.—Test Verification Program

Type testing	Test I. D.	Test purpose or objective	Test loading	Test temperature	Number of each specimen type	
Auxiliary	A-1	Material properties $(f_{tu}, f_{ty}, E, e,)$	Standard tensile test	Room temperature, 478 K, and 561 K		
Auxiliary	A-2	Verify fatigue performance of specimen	Constant amplitude	Room temperature	Eight	Seven
Auxiliary	A-3	Define elevated temperature fatigue performance	Constant amplitude	561 K	Five	
Auxiliary	A-4	Define effect of cyclic temperature	Constant amplitude	Variable temperature, 328 to 561 K	Three in-phase Three out-of-phase Three 90° phase	
Auxiliary	A-5	Define effect of elevated temperature exposure	Constant amplitude	Expose to 561 K for 500 hr. test at room temperature	Five	
Baseline	BS-1	Define fatigue life for basic load and temperature spectrum	Programmed flight-by-flight loading	Programmed flight-by-flight temperature cycles		Five
Accelerated concepts	AC-1, AC-2	Define fatigue life for accelerated test concepts	Programmed flight-by-flight loading	Room temperature		Five specimens for each concept

Table 2.—Longitudinal Tensile Properties for Ti-6Al-4V, Annealed

Sheet number—specimen I.D.	Ultimate strength	Yield strength at 0.2% offset	Indicated modulus	Elongation in 50.8 mm,
	MPa	MPa	GPa	%
Boeing material specification, minimum tensile properties at room temperature				
—	923.9	868.8	—	10
1.27-mm thickness, room temperature				
1-A	978.4	965.3	116.5	13
1-B	977.7	967.4	114.5	14
2-A	966.0	942.6	113.1	14
2-B	963.9	945.3	117.2	13
3-A	970.1	960.5	117.2	13
3-B	974.3	961.2	118.6	15
1.27-mm thickness, 478 K				
1-C	787.4	709.5	110.3	14
1-D	785.3	705.4	106.9	13
2-C	764.7	680.5	103.4	14
2-D	766.0	684.7	104.1	14
3-C	772.2	695.7	106.2	14
3-D	775.7	699.2	109.6	13
1.27-mm thickness, 561 K				
1-E	719.2	630.9	103.4	11
1-F	716.4	628.8	102.1	12
2-E	709.5	618.5	103.4	12
2-F	709.5	617.8	105.5	12
3-E	717.1	629.5	107.6	11
3-F	723.3	635.7	104.8	11
2.03-mm thickness, room temperature				
1-A	995.0	965.3	117.2	14
1-B	997.0	962.5	117.9	14
2-A	986.0	952.2	113.1	14
2-B	981.2	953.6	115.8	14
3-A	986.7	963.2	119.3	13
3-B	991.5	960.5	116.5	13
2.03-mm thickness, 478 K				
1-C	797.1	701.2	110.3	11
1-D	790.2	686.7	108.3	12
2-C	786.0	687.4	106.9	15
2-D	786.0	686.7	106.9	15
3-C	788.8	689.5	110.3	13
3-D	785.3	683.3	110.3	12
2.03-mm thickness, 561 K				
1-E	738.5	628.1	101.4	12
1-F	739.8	628.1	105.5	12
2-E	721.2	610.2	100.7	12
2-F	728.8	617.8	103.4	12
3-E	726.0	618.5	101.4	13
3-F	728.8	627.5	100.7	13

Table 3.—Auxiliary Fatigue Test Data Tests, Ti-6Al-4V Annealed, Constant Amplitude

Sheet number specimen-number	Maximum load, kN	R	Maximum stress, MPa	Cycles to failure	Failure location (fastener number)
A-2 test, room temperature, flat sheet specimen					
[a]1-1	88.96	0.06	460	27 679	6
1-2	88.96	0.06	460	30 249	5 skin, 6 stiff
1-3	71.17	0.06	368	105 215	5
1-4	71.17	0.06	368	71 222	8
1-5	80.06	0.06	414	31 011	8 skin only
1-6	80.06	0.06	414	53 170	6
1-7	62.27	0.06	322	223 914	8 skin only
1-8	62.27	0.06	322	223 995	6
A-2 test, room temperature, hat specimen					
[a]3-1	71.17	−0.35	368	21 910	6 skin only
3-2	71.17	0.06	368	79 336	6
3-11	71.17	0.06	368	79 103	7 stiff only
3-12	71.17	−0.35	368	37 065	8
3-14	62.27	−0.35	299	62 497	8
3-15	62.27	−0.35	299	77 190	5 skin, 6 stiff
3-16	62.27	−0.35	299	63 490	5 skin only
A-3 test, 561 K, flat sheet specimen					
[a]1-9	71.17	0.06	368	56 723	6
1-10	62.27	0.06	322	83 968	6 skin only
1-11	62.27	0.06	322	88 199	5 skin only
1-12	57.82	0.06	299	177 296	8
1-13	57.82	0.06	299	98 594	7 skin only
A-4 test, 327 to 561 K, cyclic temperature, flat sheet specimen, 0° (in) phase					
[a]1-14	71.17	0.06	368	72 520	4 skin, 1 stiff
1-15	71.17	0.06	368	(32 200)	Compression failure
1-19	71.17	0.06	368	77 366	5
-23	71.17	0.06	368	50 633	7 skin, 6 stiff
A-4 test, 90° phase					
1-16	71.17	0.06	368	47 577	5
1-17	71.17	0.06	368	57 714	6
1-18	71.17	0.06	368	55 695	5
A-4 test, 180° phase					
1-20	71.17	0.06	368	52 930	5 skin, 4 stiff
1-21	71.17	0.06	368	66 989	8
1-22	71.17	0.06	368	63 602	5
A-5 test, room temperature, 500 hr, 561 K prior exposure, flat sheet specimen					
2-34	71.17	0.06	368	59 337	6 skin only
2-35	62.27	0.06	322	79 951	6 skin only
2-36	71.17	0.06	368	54 445	5 skin only
2-37	62.27	0.06	322	544 305	4
2-38	57.82	0.06	299	192 089	8 stiff only

[a]Test specimen used for static survey prior to fatigue testing

Table 4.—Fatigue Test Data, Baseline Flight-by-Flight Tests

Sheet number—specimen number	$S_{1g,d}$ MPa	Flights to failure	Failure location (fastener number, flight type)
BS-1 test, cyclic temperature, flight-by-flight loads, hat specimen			
[a]3-3	207	33 828	7 skin and stiffener (100th flt)
3-5	207	51 682	7 skin and stiffener (100th flt)
3-7	207	(33 115)	failed in compression
3-13	207	90 334	5 skin and stiffener (100th flt)
3-18	207	44 496	5 skin and stiffener (100th flt)
Median = 48 089 flights, log-average = 51 487 flights			

[a]Test specimen used for static survey prior to fatigue testing

Table 5.—Fatigue Test Data, Accelerated Flight-by-Flight Tests

Sheet number—specimen number	$S_{1g,d}$ MPa	Flights to failure	Failure location (fastener number, flight type)
AC-1 test, flight-by-flight loads, hat specimen, room temperature test, heat soaked 500 hr at 561 K			
3-4	207	65 304	5 skin and stiffener (5th flt)
3-6	207	80 000	5 skin and stiffener (basic flt)
3-8	207	39 465	7 skin and stiffener (5th flt)
3-9	207	33 765	4 skin and stiffener (basic flt)
3-10	207	47 501	6 skin and stiffener (100th flt)
Median = 47 501 flights, log-average = 50 569 flights			
AC-2 test, flight-by-flight loads, hat specimen, room temperature test			
3-22	207	54 113	6 skin and stiffener (basic flt)
3-23	207	62 537	6 skin and stiffener (100th flt)
3-20	207	50 931	6 skin and stiffener (5th flt)
3-19	207	65 463	5 skin and stiffener (100th flt)
3-21	207	69 290	7 skin and stiffener (basic flt)
Median = 62 537 flights, log-average = 60 064 flights			

Table 6.—Chemical Composition, Heat Treatment, and Surface Finish of Ti-6Al-4V Annealed (Information Supplied by Vendor)

Element	Percent weight composition	
	1.27-mm thickness heat N-0548	2.03-mm thickness heat N-1783
C	0.026	0.026
Fe	0.08	0.12
N	0.012	0.016
Al	5.8	5.7
Va	4.0	4.0
H	0.009	0.006
O	0.12	0.11
[a]Other impurities	[a]0.40	[a]0.40
Titanium	Balance	Balance

[a]Not required in qualification report, specification maximum given. Any individual element shall not exceed 0.10%.

Heat treatment: (specification)
    1005 to 1061 K for 15 min to 8 hr.
    Cool at less than 644 K per hour to
    811 K, cooling optional.

Surface finish: (specification)
    All sheet shall have a surface appearance equivalent
    to a 2D finish for commercial corrosion-resistant
    steel and shall have a 32 RHR or better surface
    roughness.

    All sheet shall have been sanded and subsequently
    pickled.
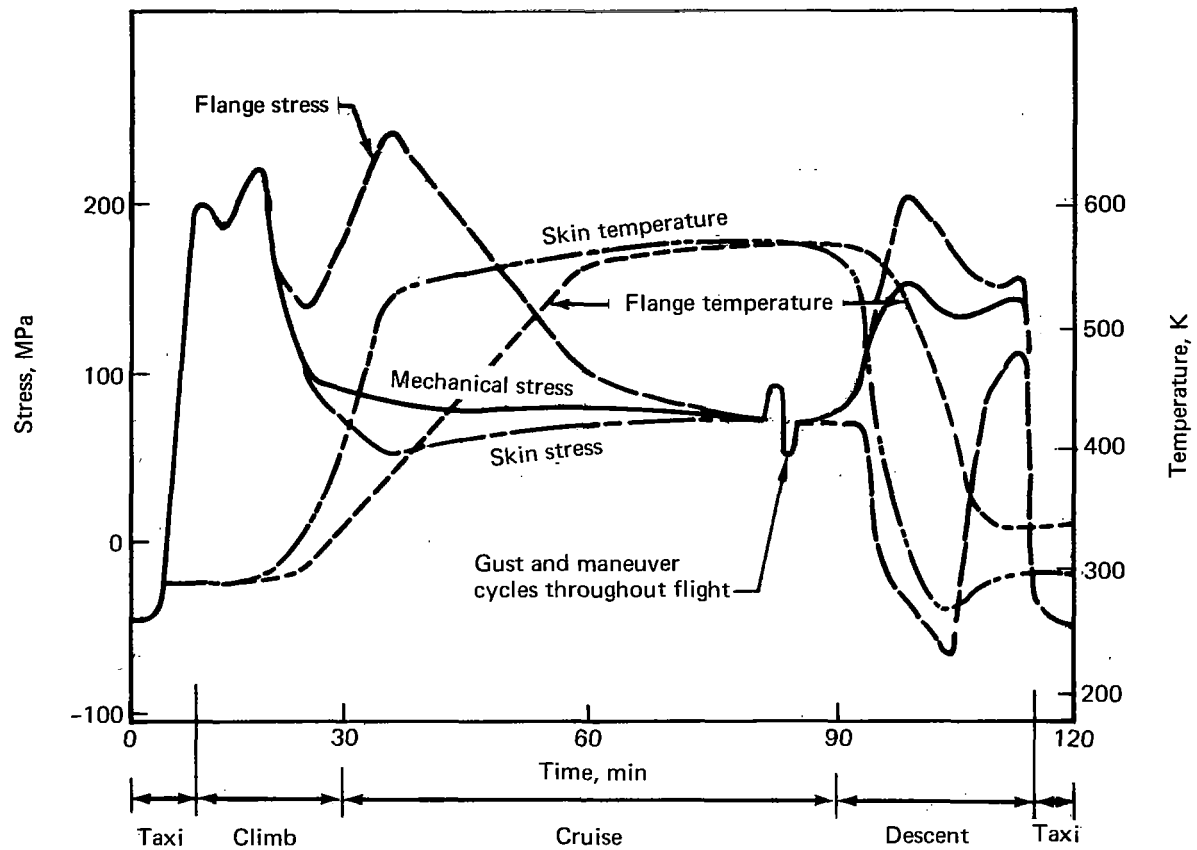
Figure 1.—Typical Wing Lower Surface Stress History

O Rivet, hi-squeeze installation
□ Bolt, "Hi-Lok"
∇ Bolt, "Taper-Lok"

S_{max} at R = 0.06 for 10^5 cycles life

$\dfrac{S_{max} \text{ exposed}}{S_{max} \text{ unexposed}}$

Type specimen:
   Simulated skin-
   stiffener attachment
Exposure:
   Temperature = 561 K
   Load = 0

Exposure time, hr

(a) Exposure to Temperature

∇ Rivet, A-286 material, gun-driven installation
O Rivet, A-286 material, squeeze installation
□ Rivet, Ti-6Al-4V material, squeeze installation

S_{max} at R = 0.06 for 10^5 cycles life

$\dfrac{S_{max} \text{ exposed}}{S_{max} \text{ unexposed}}$

Type specimen:
   Lap shear joint

Exposure:
   Temperature:
      Open symbols
      = 561 K
      Closed symbols
      = 505 K
   Stress = 207 MPa

Exposure time, hr

(b) Exposure to Load and Temperature

Figure 2.—Fatigue Performance of Ti-6Al-4V Built-Up Structure After Exposure

25

$$S_{max}' = \frac{S_{max}}{\hat{\eta}} \left.\vphantom{\frac{S_{max}}{\hat{\eta}}}\right\}$$
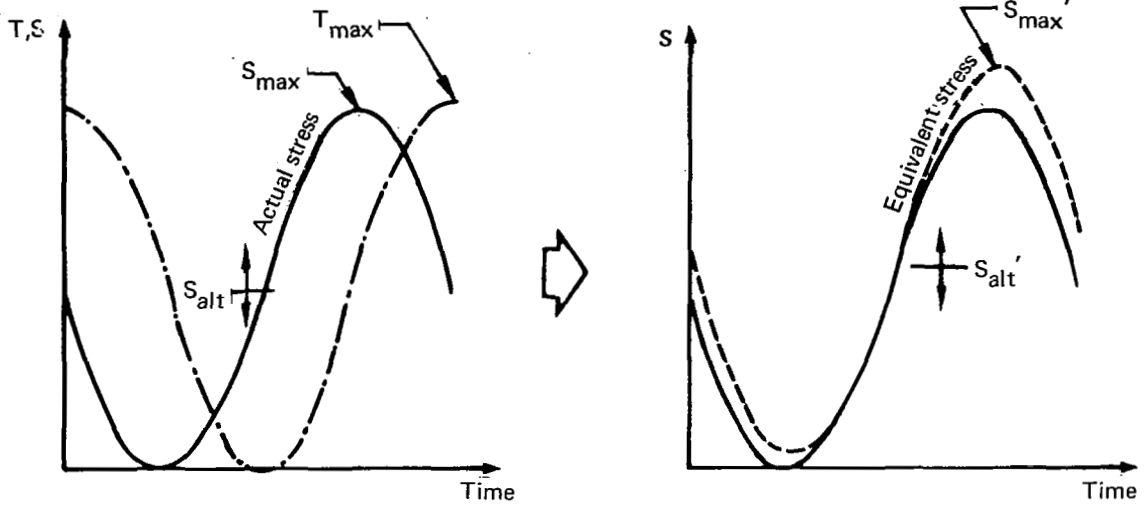
$$S_{alt}' = \frac{S_{alt}}{\bar{\eta}}$$

where:

$\hat{\eta} = E_{ET}/E_{RT}$ the modulus degradation ratio for the temperature at S_{max}

$\bar{\eta} = \overline{E_{ET}/E_{RT}}$ the average modulus degradation ratio for T_{max} and T_{min} $\bar{\eta} = \left(\dfrac{\hat{\eta}+\check{\eta}}{2}\right)$

$\check{\eta} = E_{ET}/E_{RT}$ the modulus degradation ratio for the temperature at S_{min}

Example: 10 ± 10 stress cycle

Actual stress	T phase difference	Temperature, K		Modulus degradation		Equivalent stress	
		at S_{max}	at S_{min}	$\hat{\eta}$	$\check{\eta}$	S_{max}'	S_{alt}'
10 ± 10	Const.	300	300	1.00	1.00	20.0	10.0
	180°	300	561	1.00	0.85	20.0	10.9
	90°	432	432	0.92	0.92	21.8	10.9
	0°	561	300	0.85	1.00	23.5	10.9
10 ± 10	Const.	561	561	0.85	0.85	23.5	11.8

Figure 3.—Equivalent Stress Cycle Formulation

$\diamondsuit$ (1.60-mm thickness) $\left.\right\}$ $\dfrac{S_{ET}}{S_{RT}}$ at 10^5 cycles, $R = -1$, 0, and 0.538 (ref. 8)

∇ (3.18-mm thickness)

S

$\dfrac{E_{ET}}{E_{RT}}$ (ref. 9)

$\dfrac{Smax_{ET}}{Smax_{RT}}$ at 10^5 cycles and $\dfrac{E_{ET}}{E_{RT}}$

1.0

.9

.8

.7

6

300   400   500   600
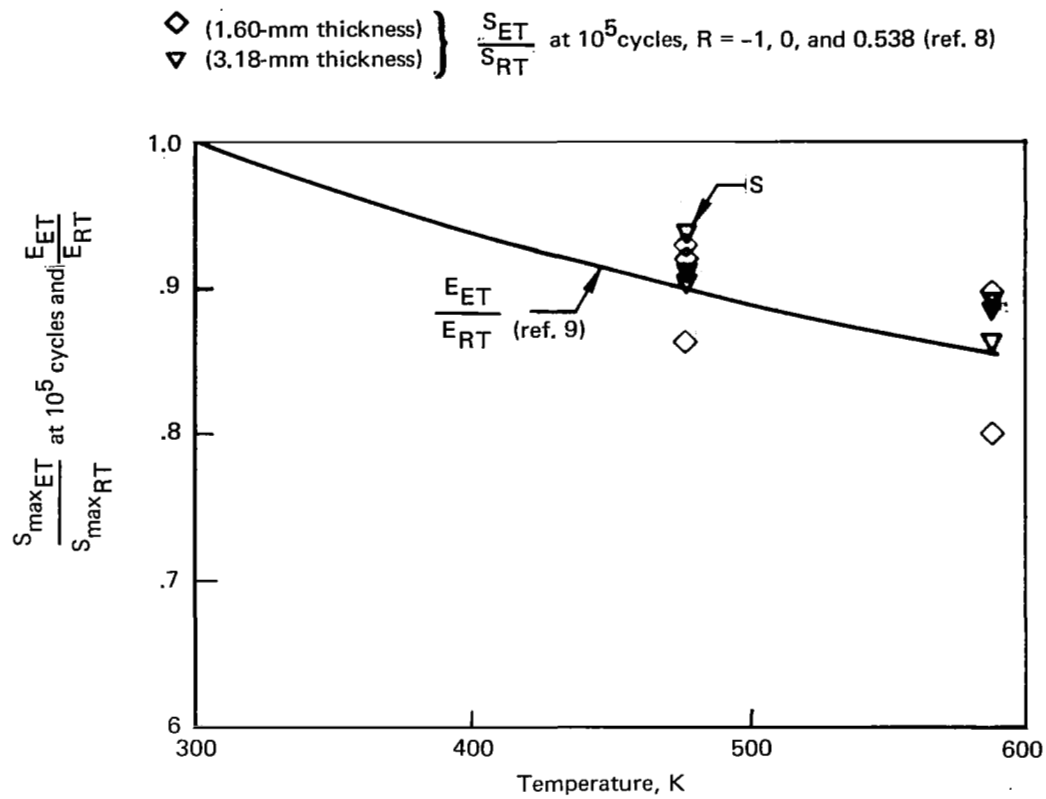
Temperature, K

Figure 4.—Correlation of Fatigue Strength and Elastic Modulus Reductions With Temperature for Ti-6Al-4V, STA

27
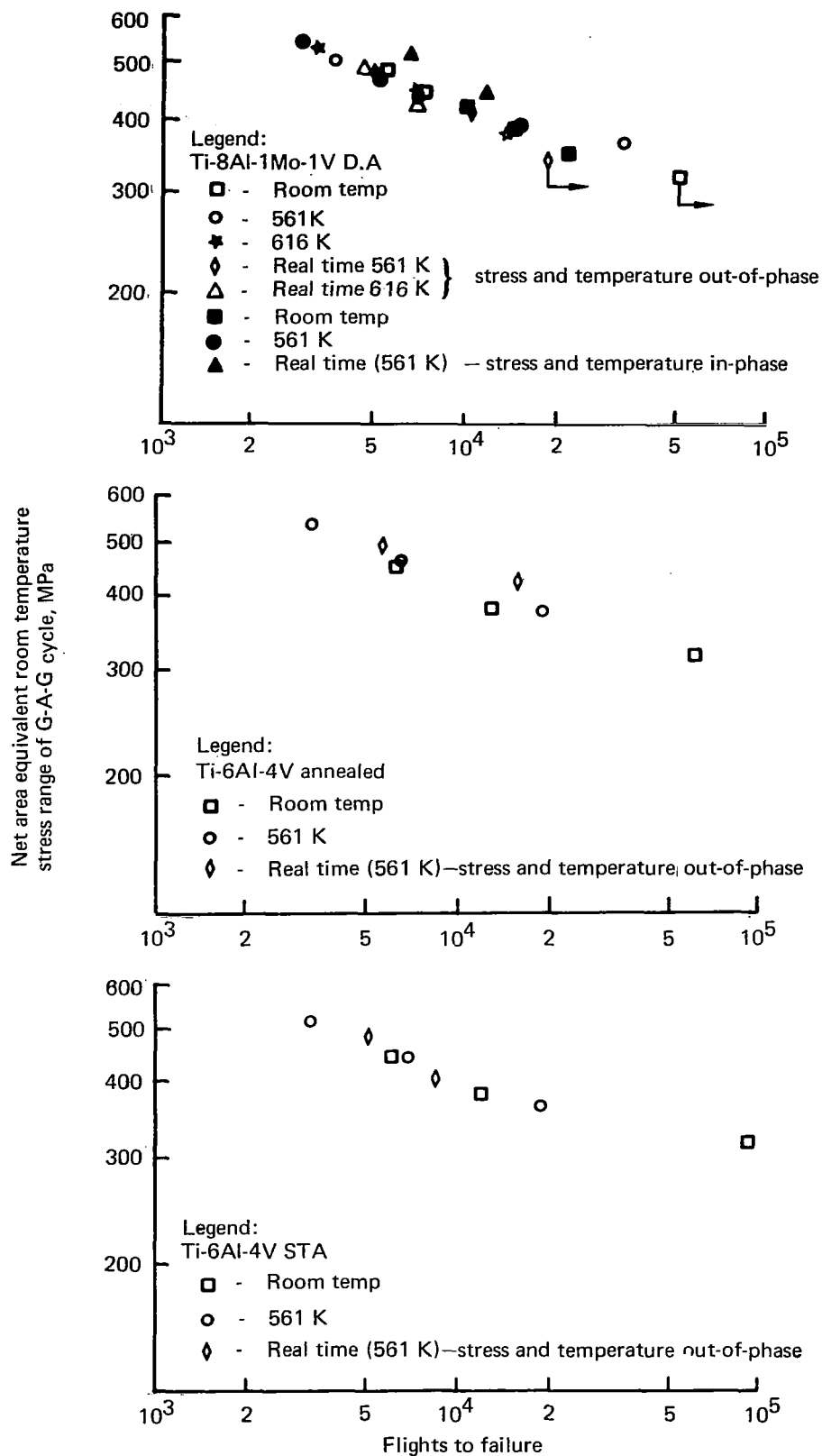
Figure 5.—Equivalent Room Temperature Stress-Versus-Life Correlation for Flight-by-Flight Fatigue Tests at Room Temperature, 561 and 616 K (Ref. 6)

28

Skin

Stiffener, 1.27-mm sheet

Skin 2.03-mm sheet

Stiffener

A

A

A-A

(a) Flat-Sheet Specimen

Skin

Stiffener, 1.27-mm sheet

Skin 2.03-mm sheet

Stiffener

B

B

B-B

(b) Hat Specimen
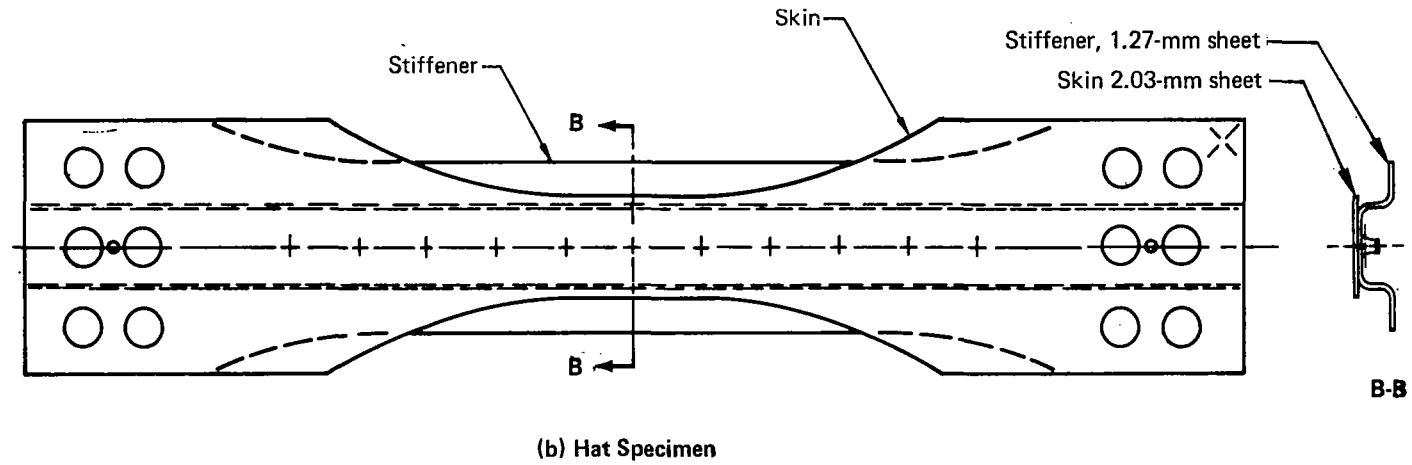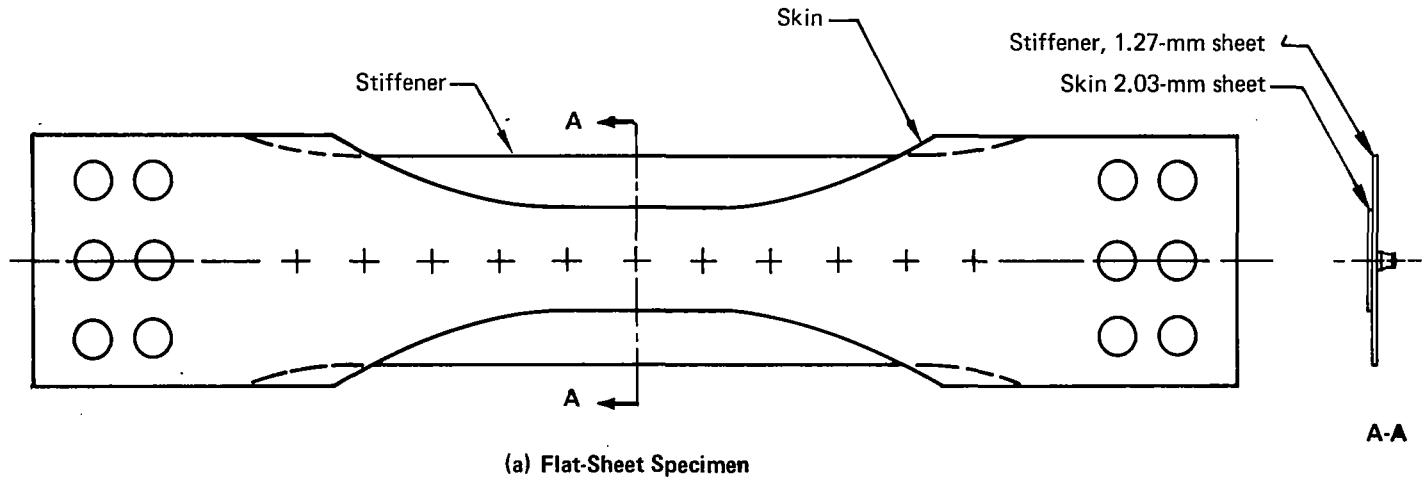
Figure 6.—Fatigue Specimen Configurations
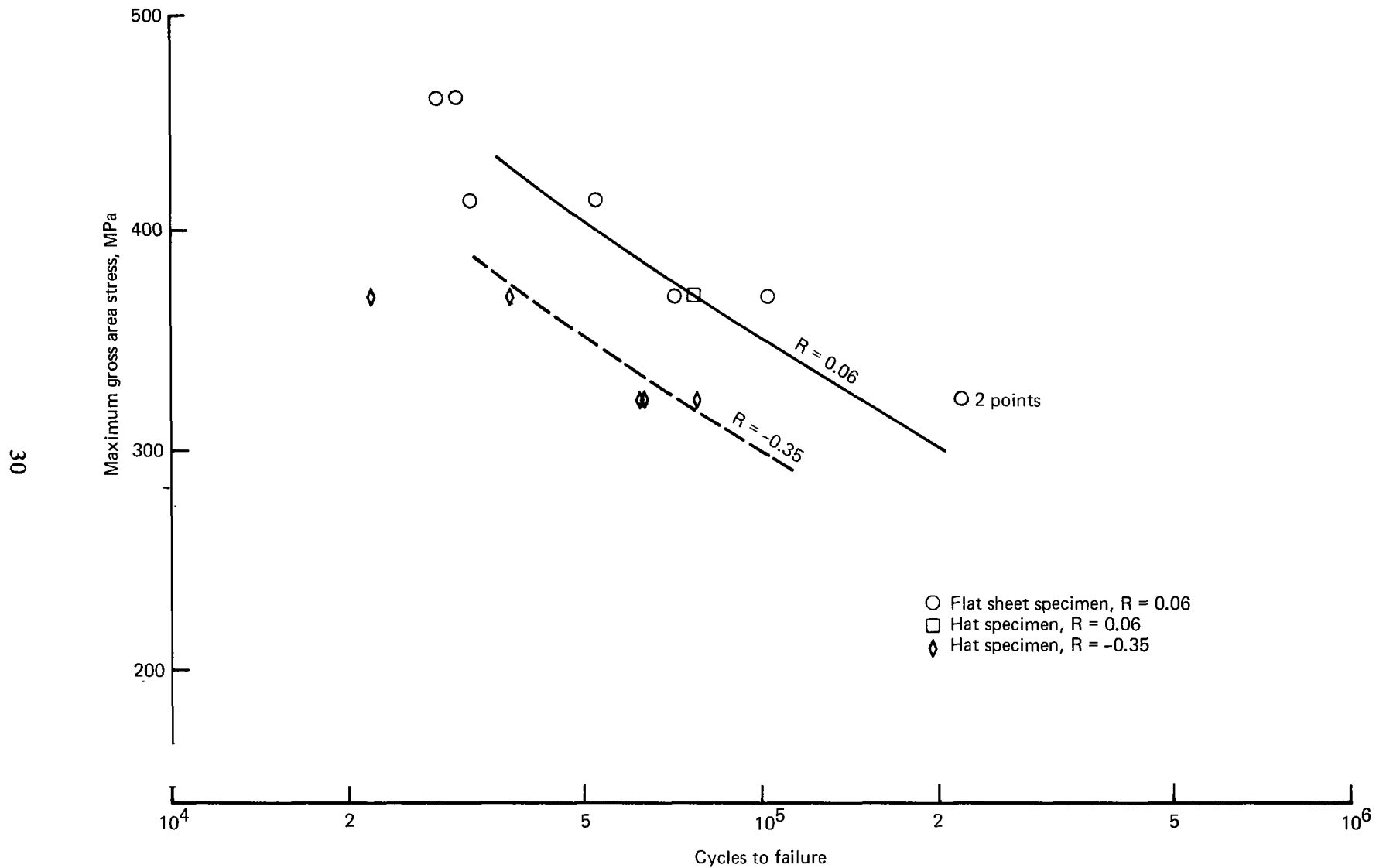
Figure 7.—Results of Constant-Amplitude Fatigue Tests at Room Temperature, Annealed Ti-6Al-4V Sheet (A-2)
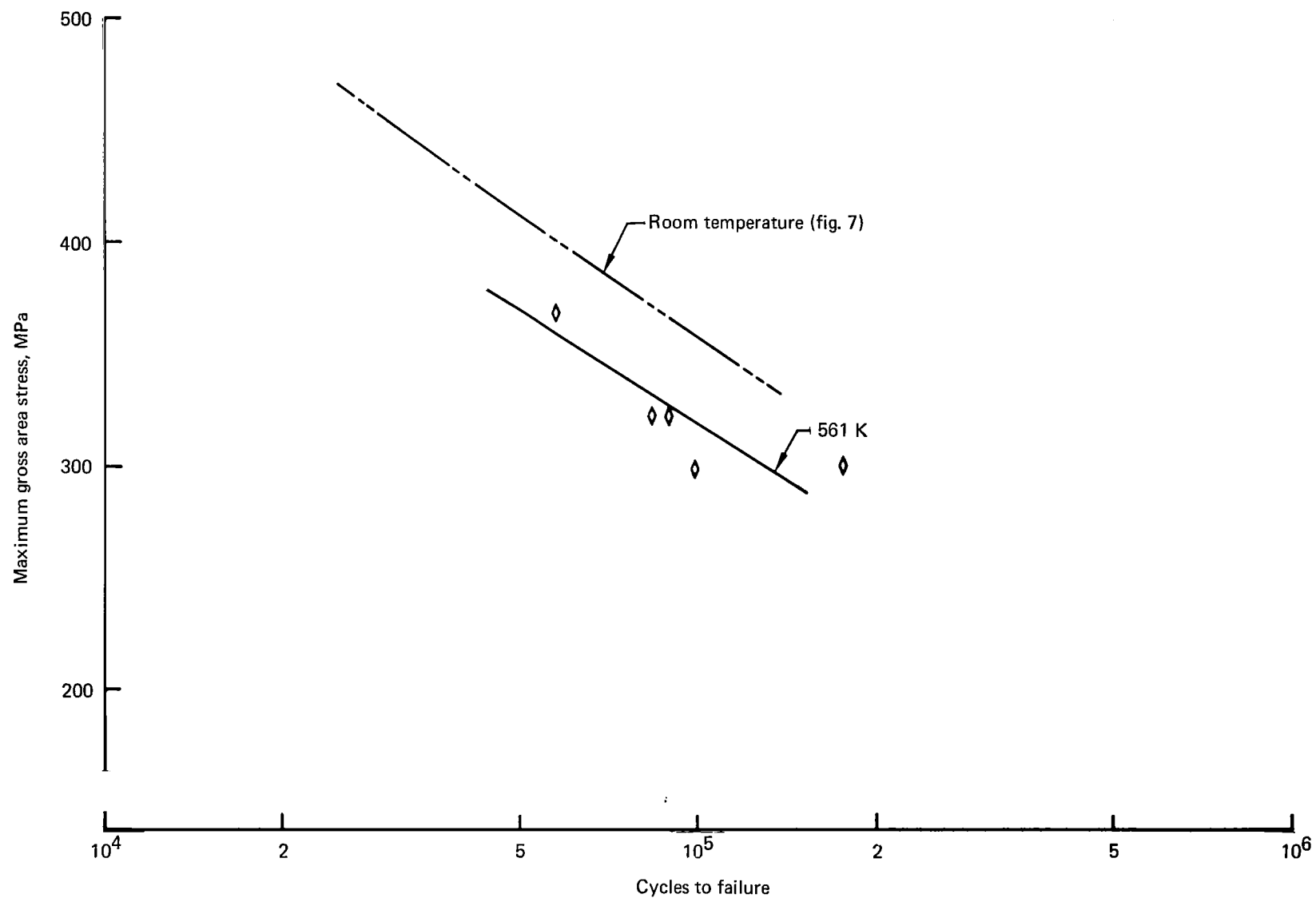
Figure 8.—Results of Constant-Amplitude Fatigue Tests at 561 K, Annealed Ti-6Al-4V, R = 0.06 (A-3)
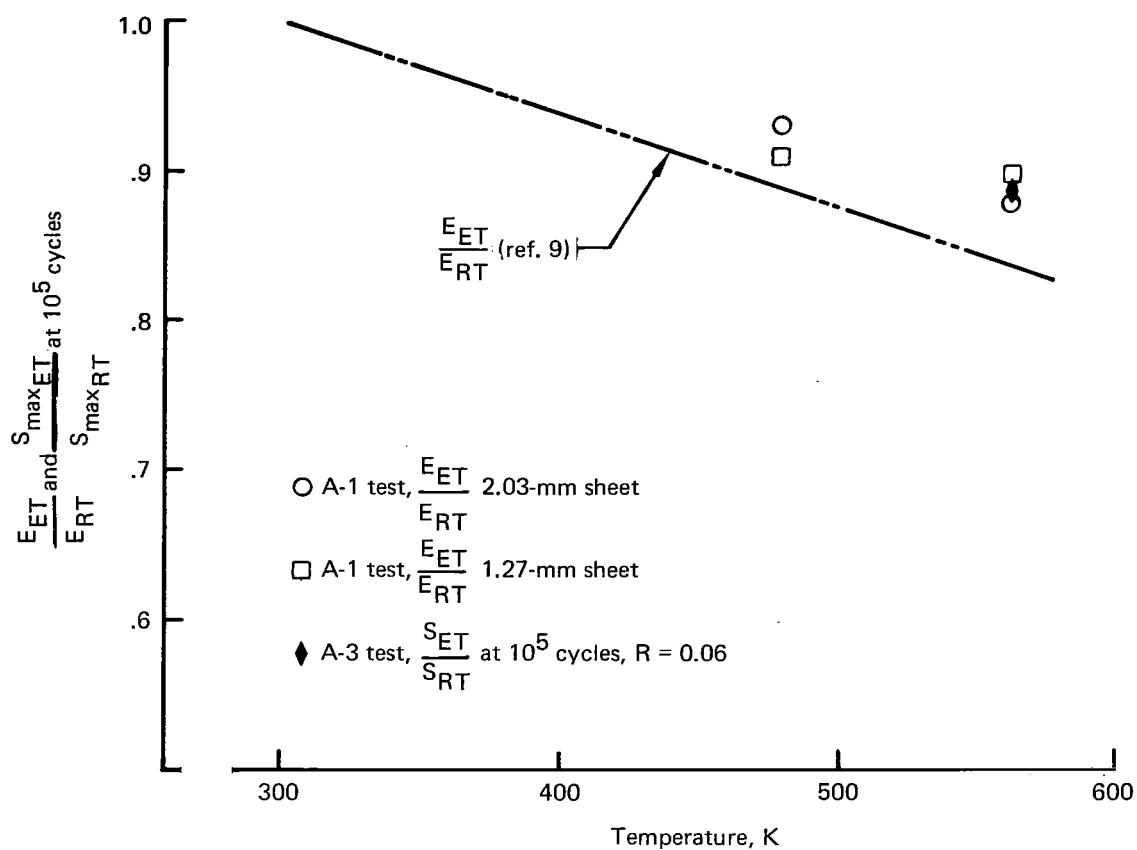
Figure 9.—Correlation of Fatigue Strength and Elastic Modulus With Elevated-Temperature for Constant-Amplitude Fatigue Tests of Annealed. Ti-6Al-4V
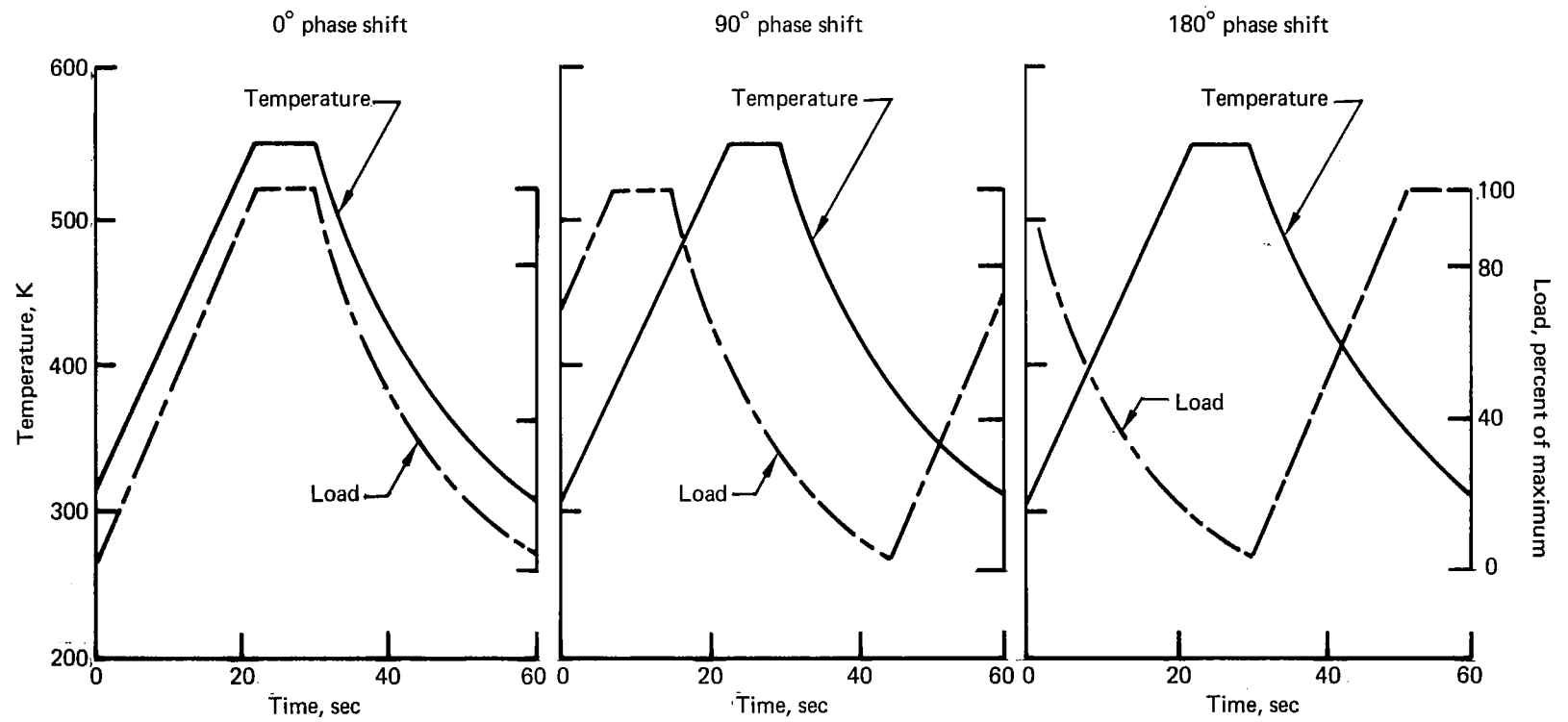
Figure 10.—A-4 Load and Temperature Profiles
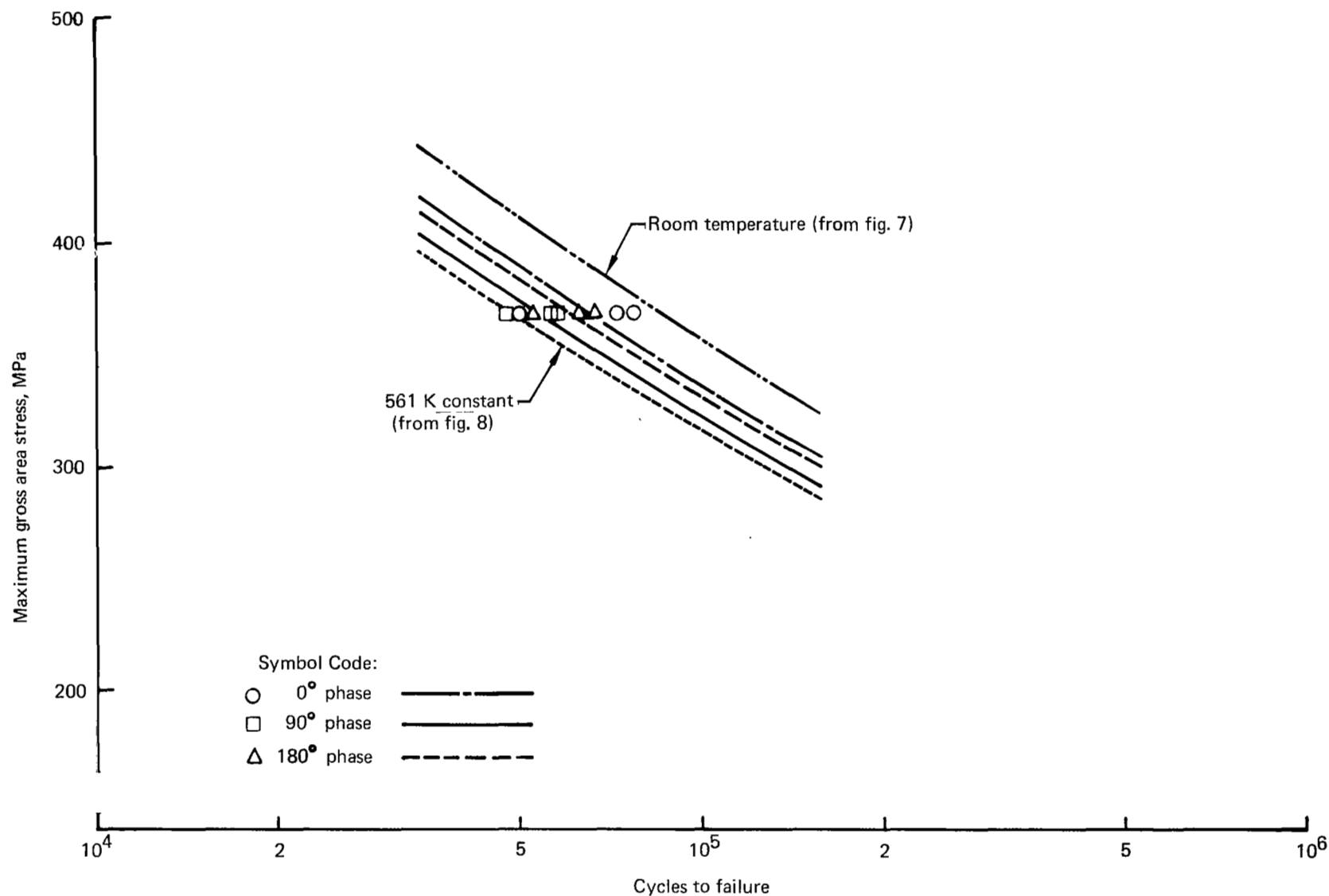
*Figure 11.—Effect of Temperature Phasing on Constant-Amplitude Fatigue Lives of Annealed Ti-6Al-4V,
R = 0.06 (A-4)*
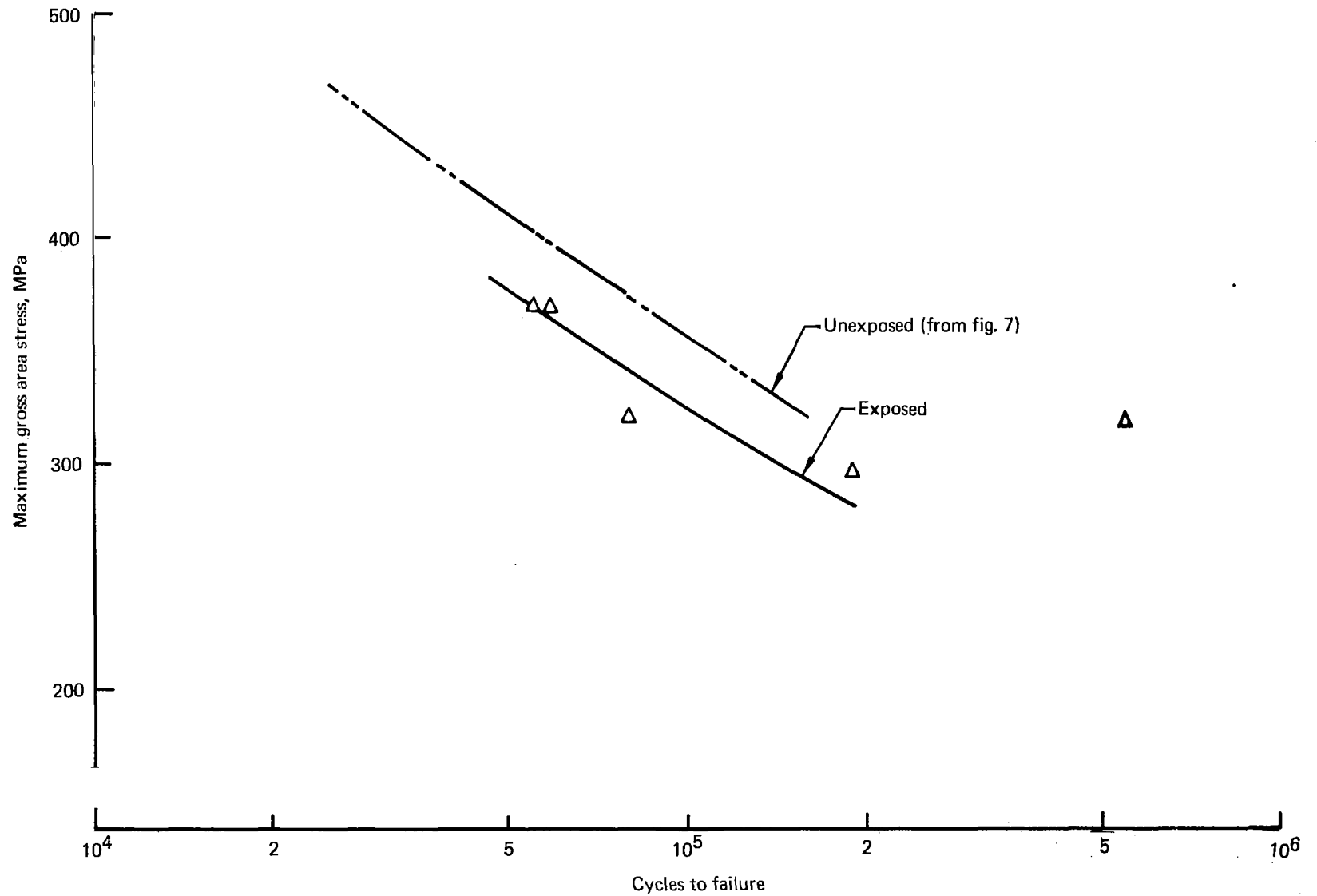
Figure 12.—Effect of Exposure to 561 K for 500 Hours on Room-Temperature Fatigue Strength
of Ti-6Al-4V, R = 0.06 (A-5)
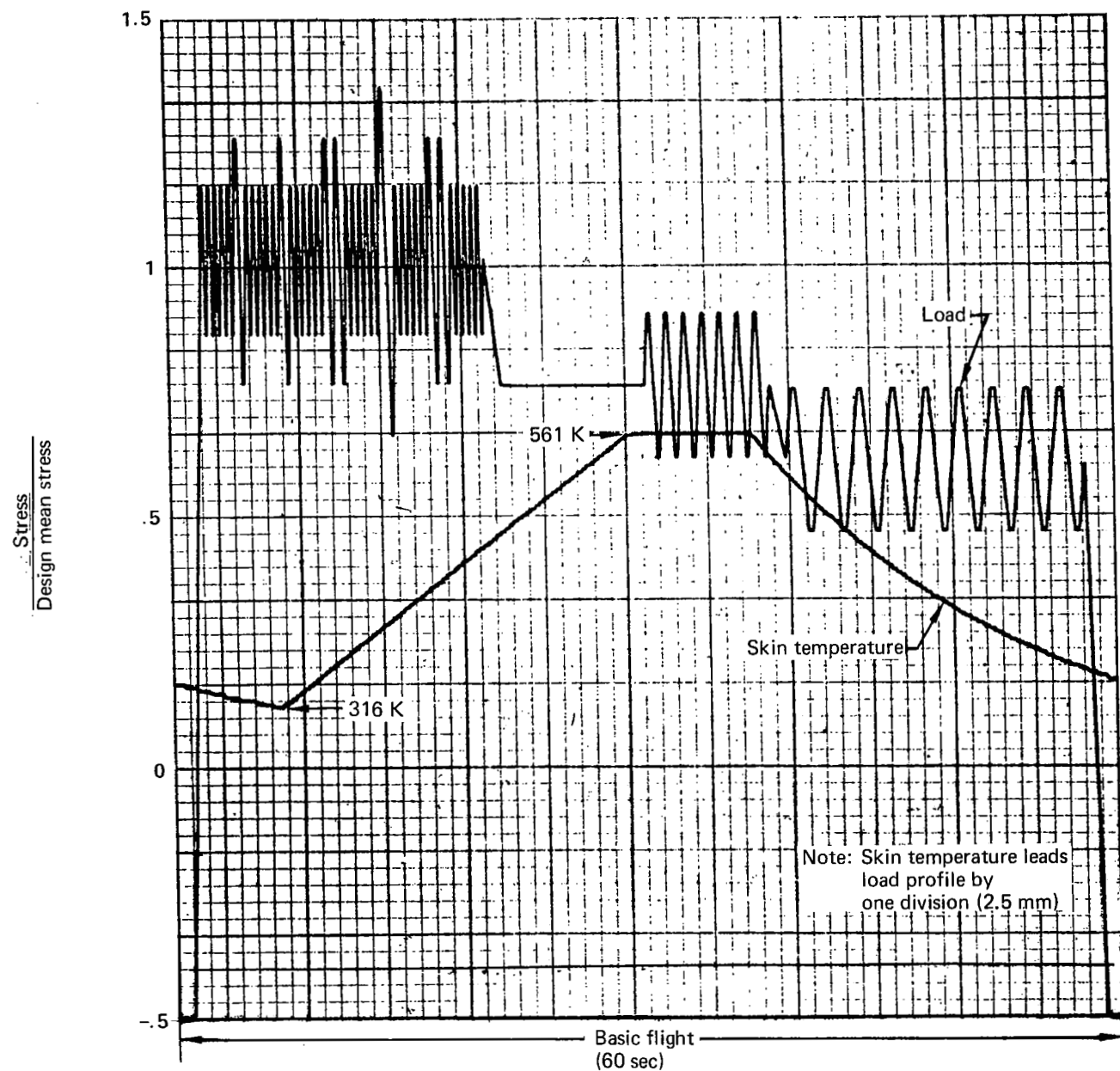
Figure 13.—Basic Flight Load and Skin Temperature Controller Profiles
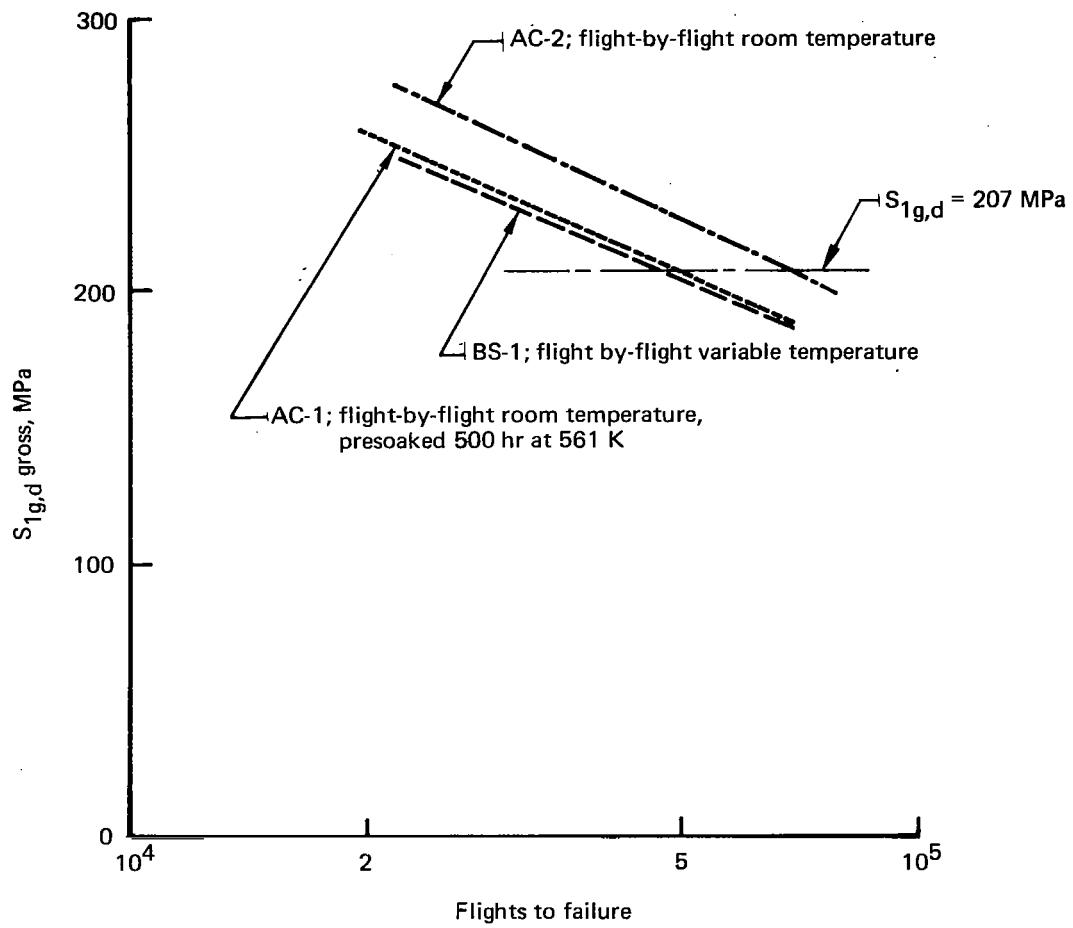
Figure 14.—Predicted Lives of Flight-by-Flight Tests
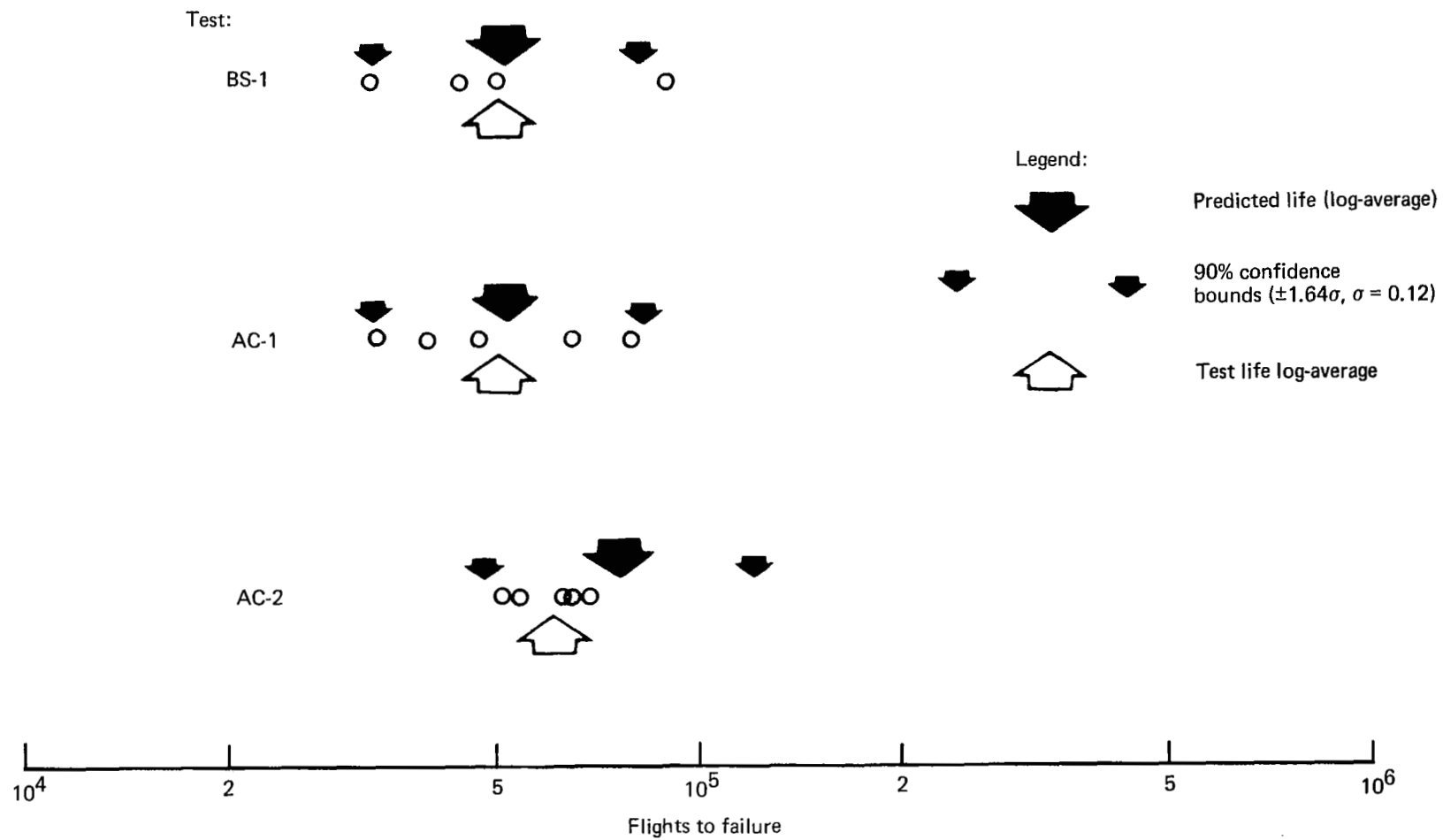
Figure 15.—Flight-by-Flight Test Results
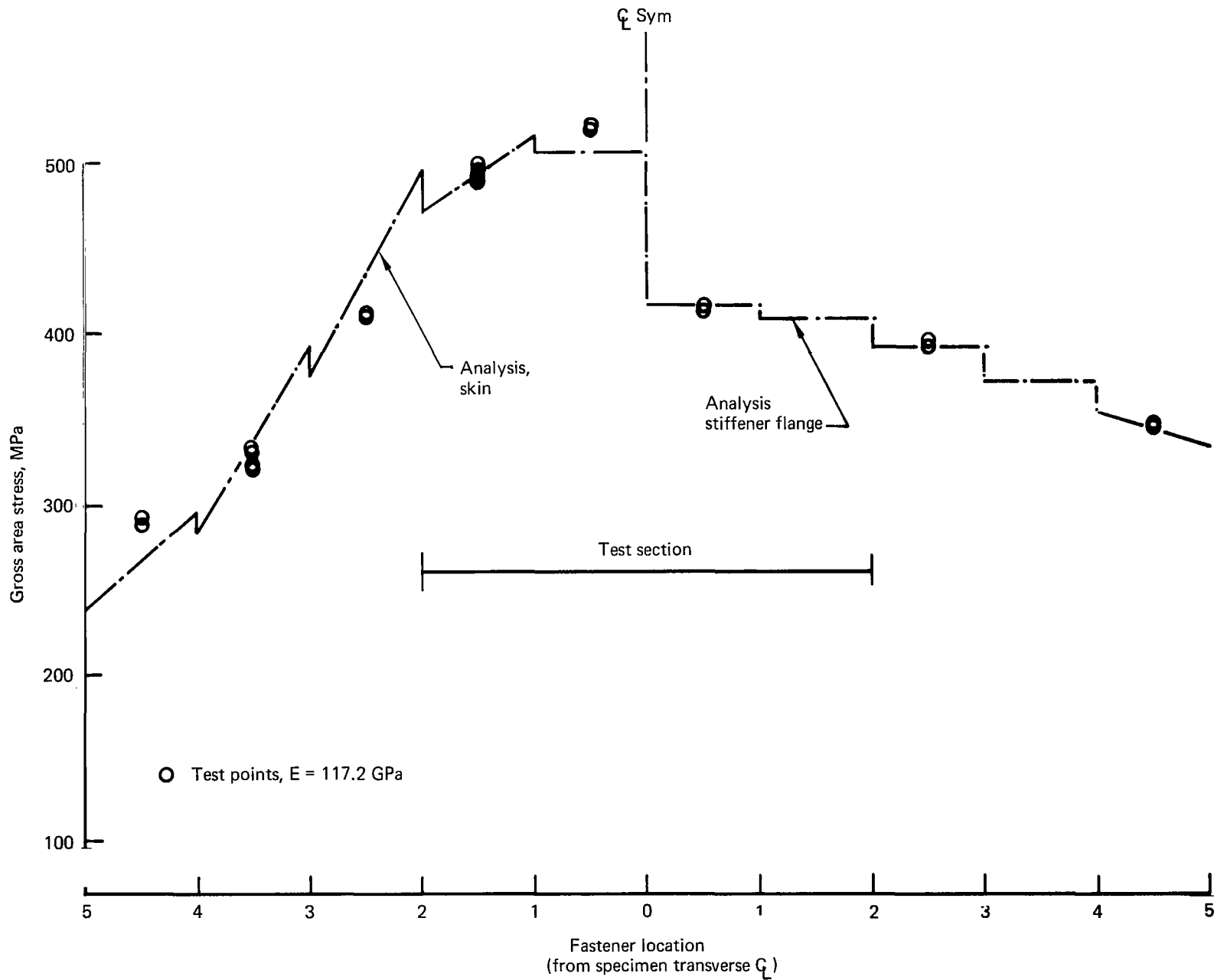
Figure 16.—Stress Analysis of Flat-Sheet Specimen at a Load of 87 kN
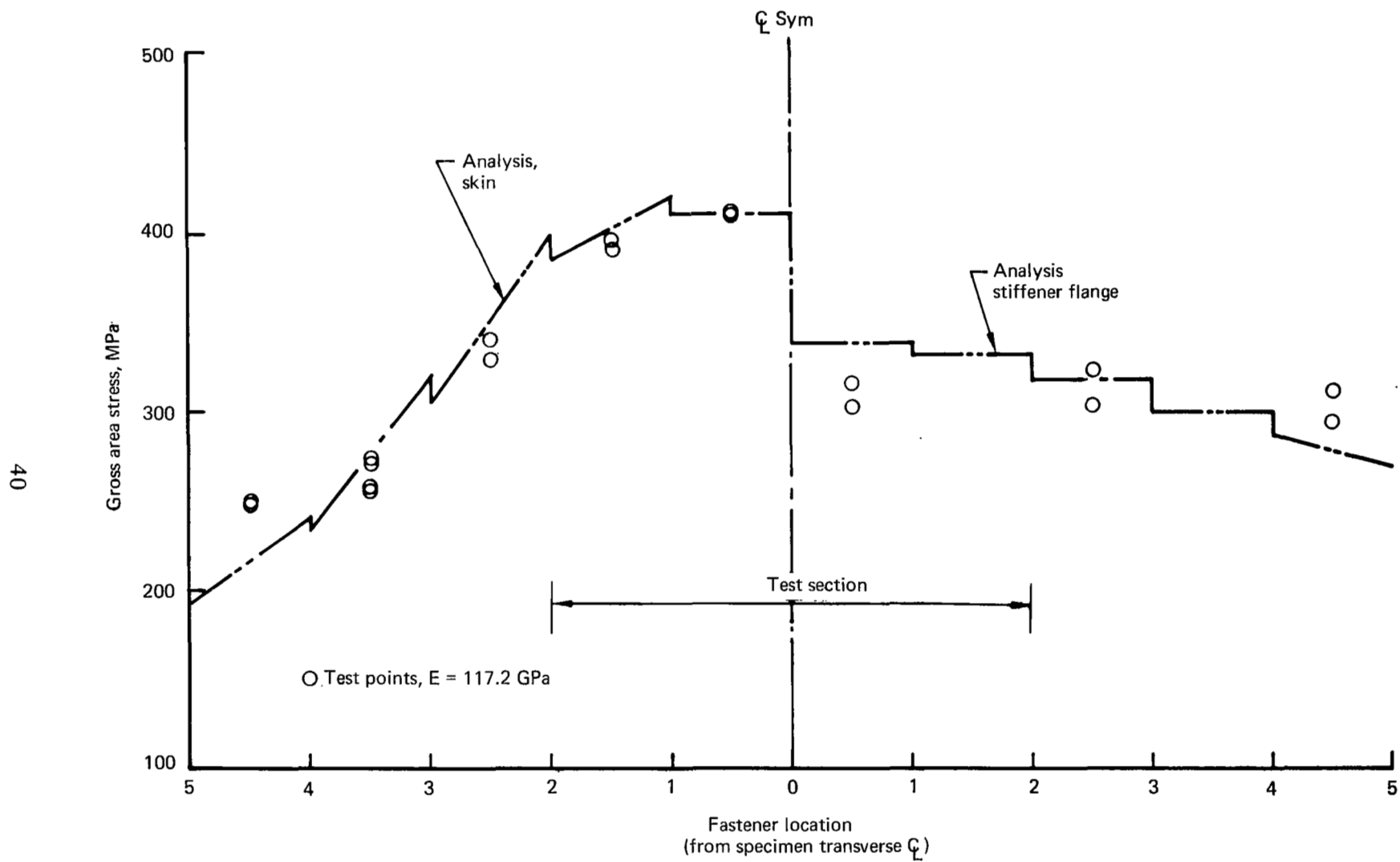
Figure 17.—Stress Analysis of Hat Specimen at a Load of 71 kN
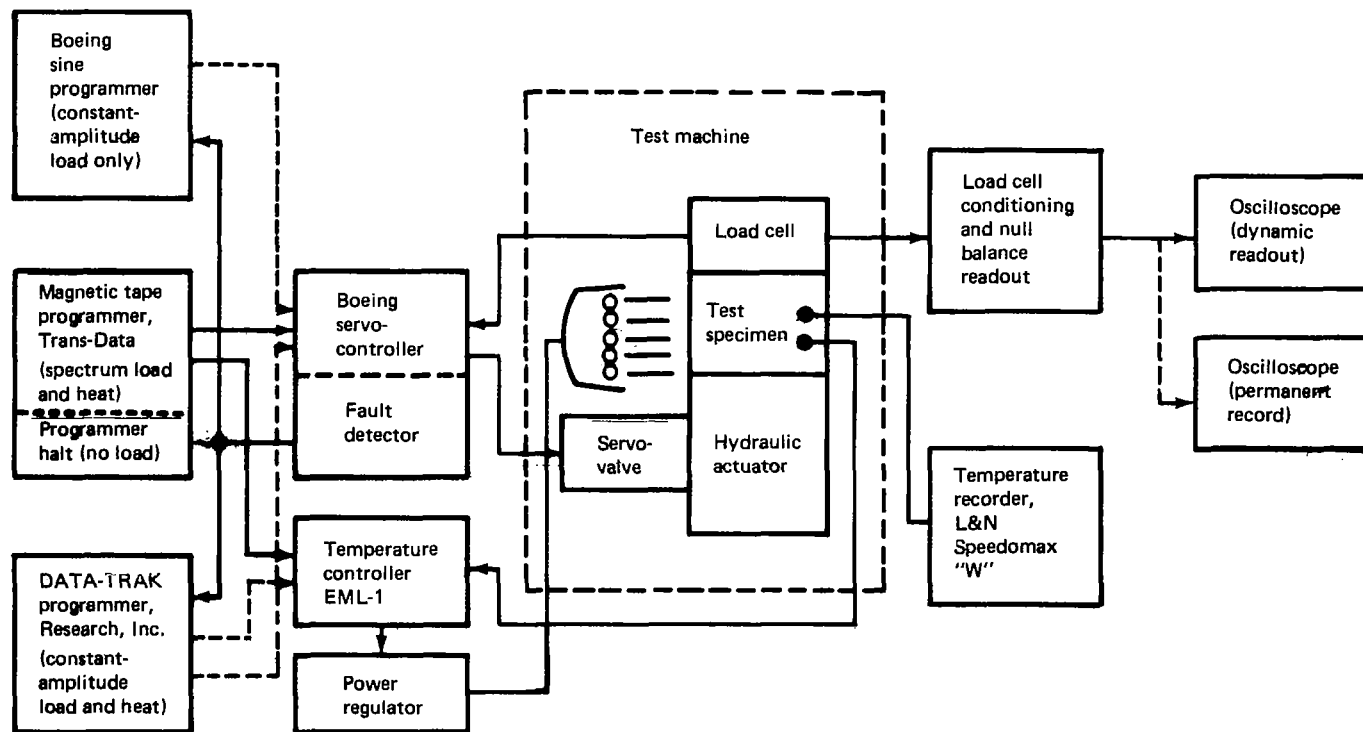
Figure 18.—Block Diagram of Test Control and Monitoring System

Figure 19.—Load Frame Arrangement
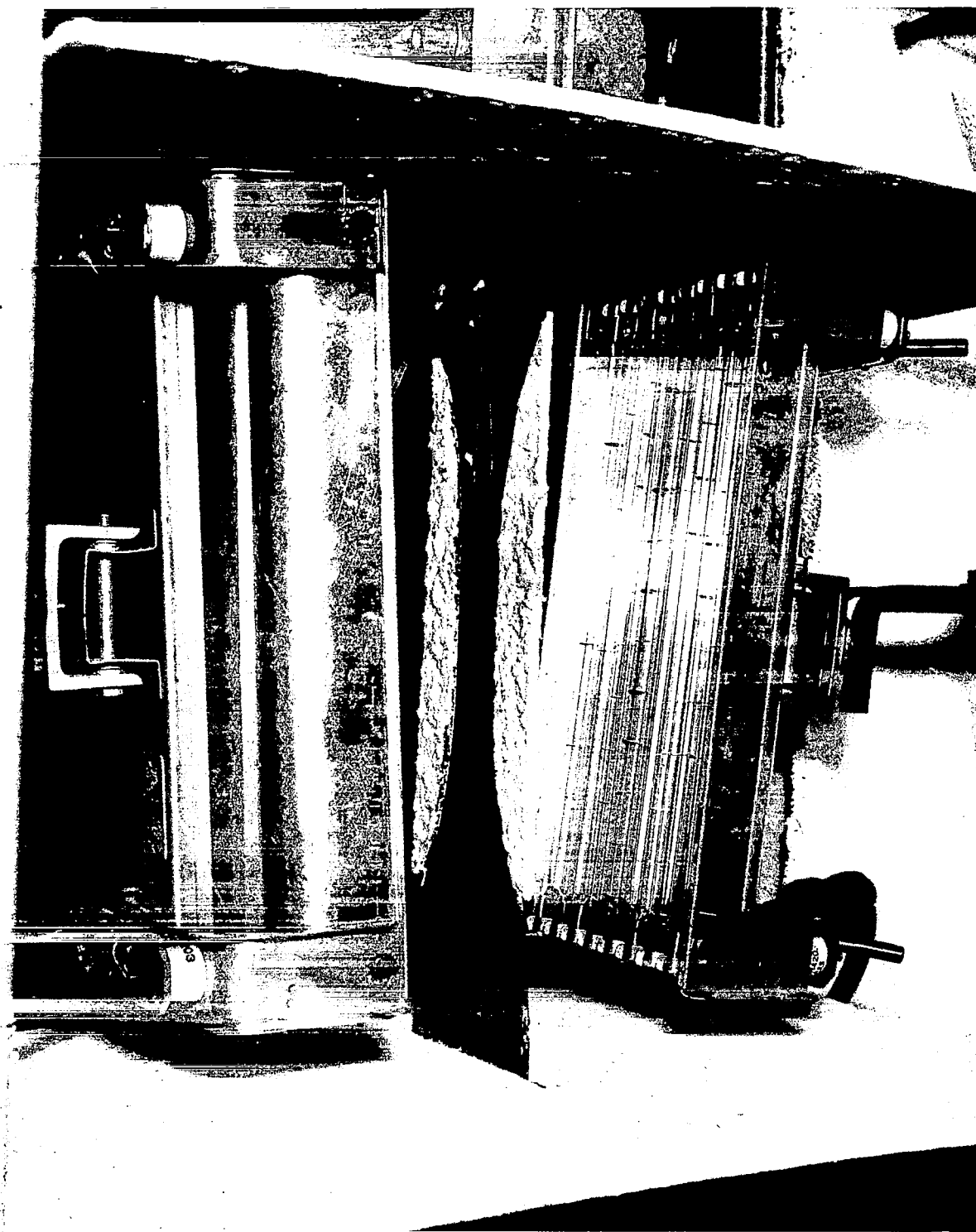
Figure 20.—Typical Test Setup (A-3 Shown)
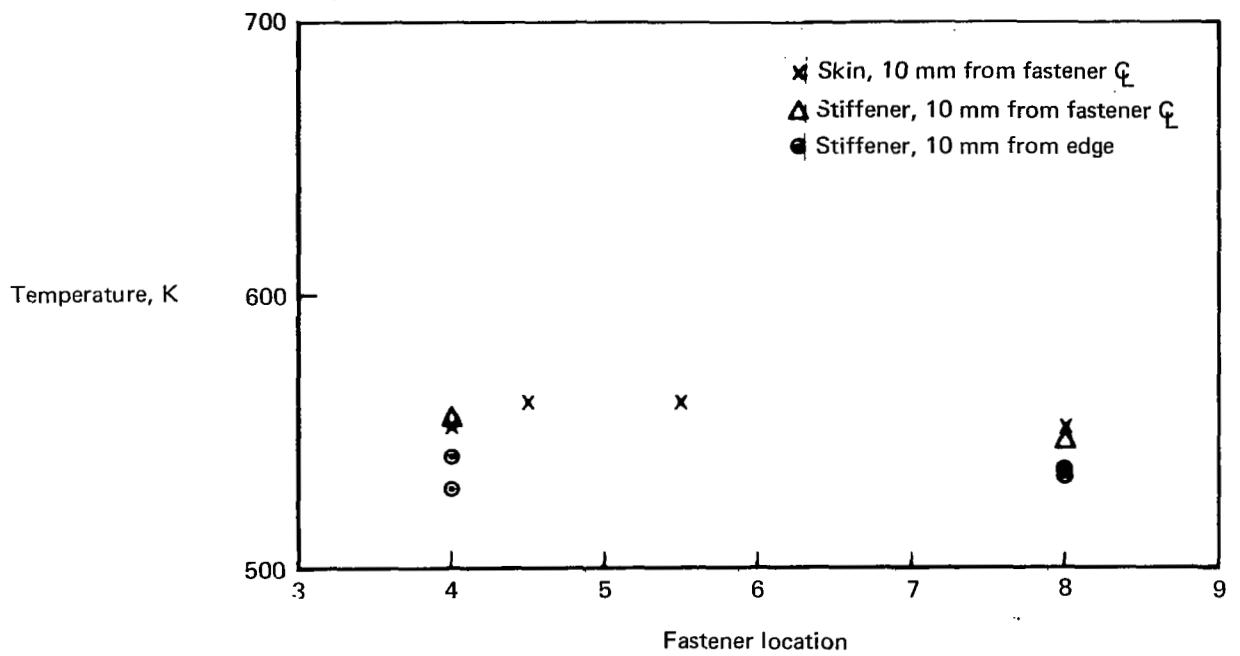
Figure 21.—Temperature Distribution for Constant-Temperature Fatigue Tests
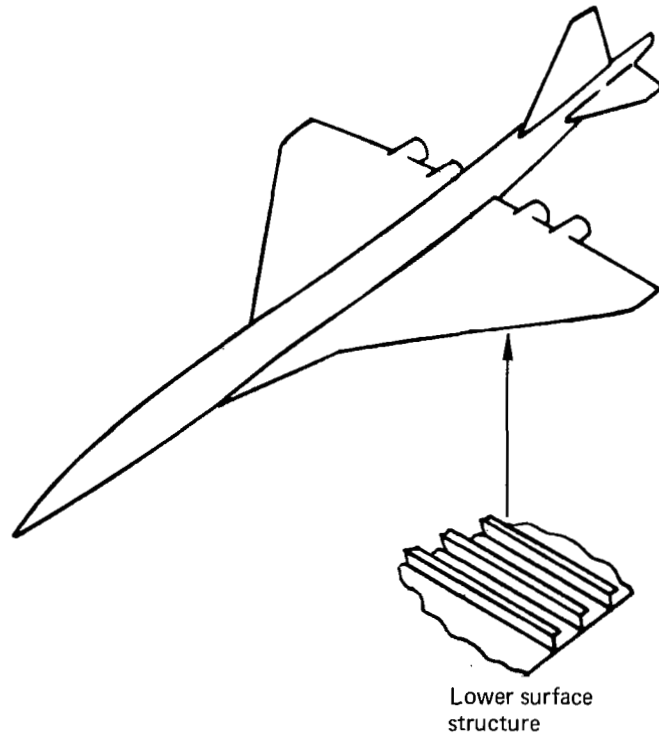
Thermal stress, MPa

Temperature, K

Lower surface
structure

Time, min
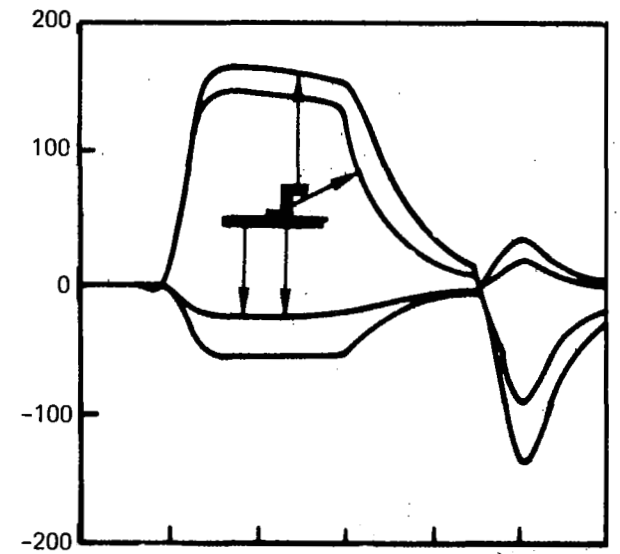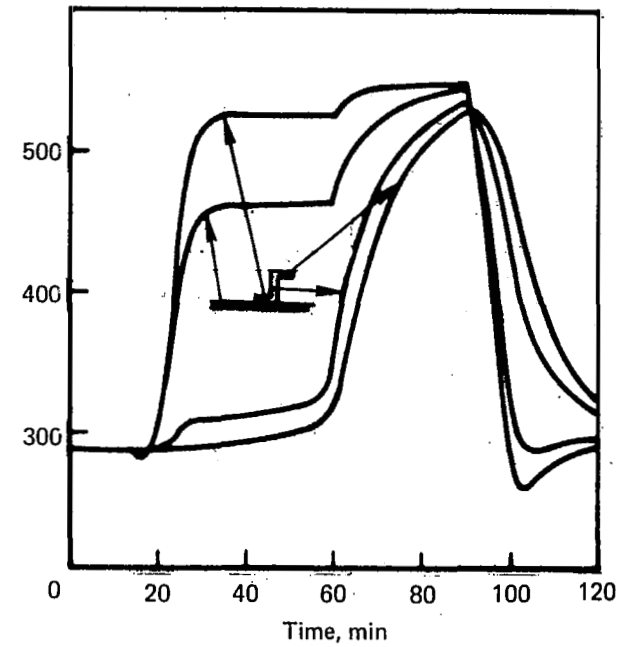
Figure 22.—Thermal Analysis for Wing Lower Surface Structure of Assumed Mach 3 Transport

Flight-by-flight
test specimen
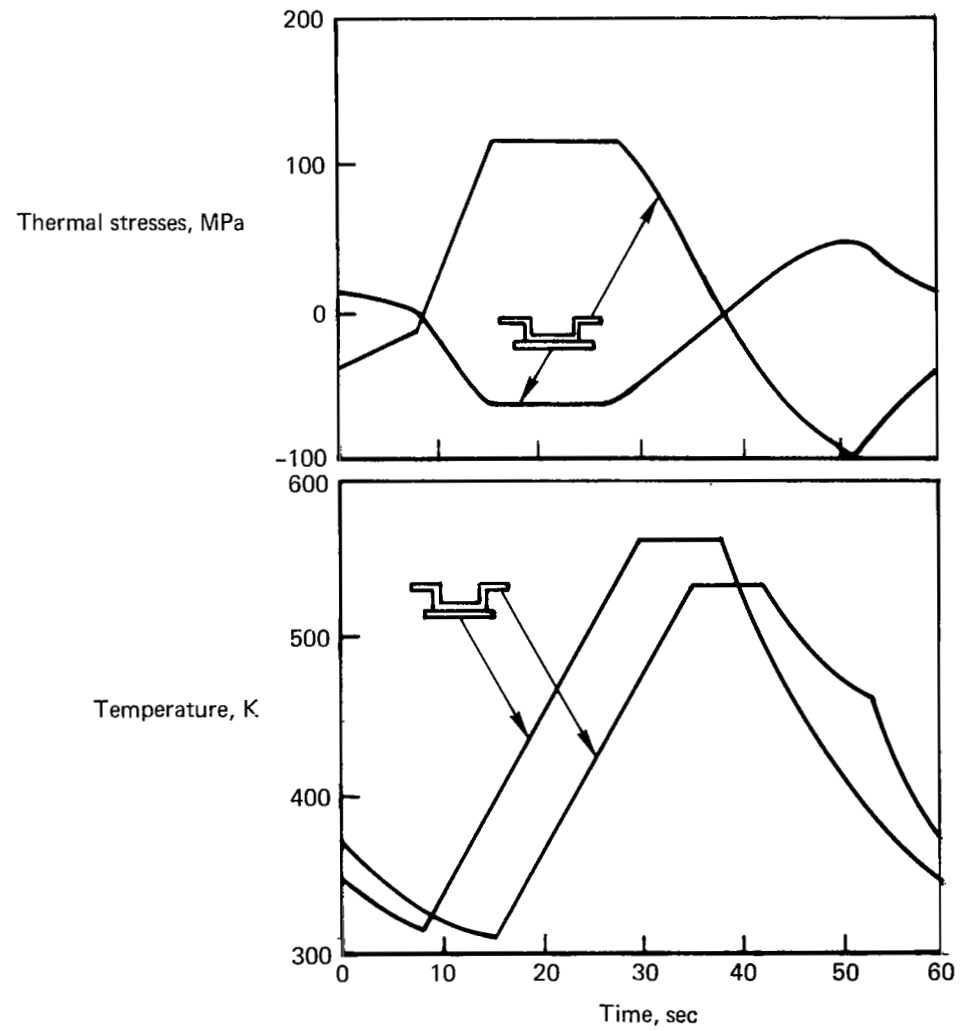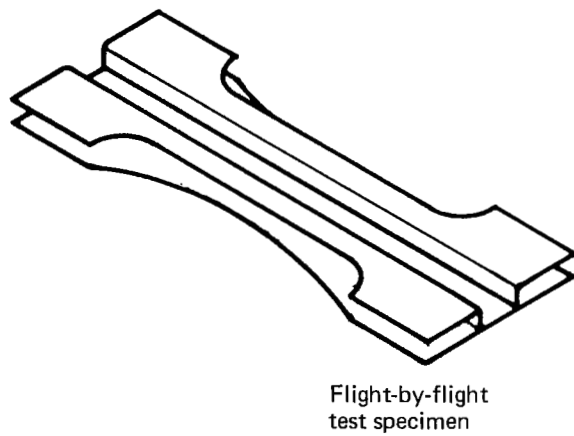
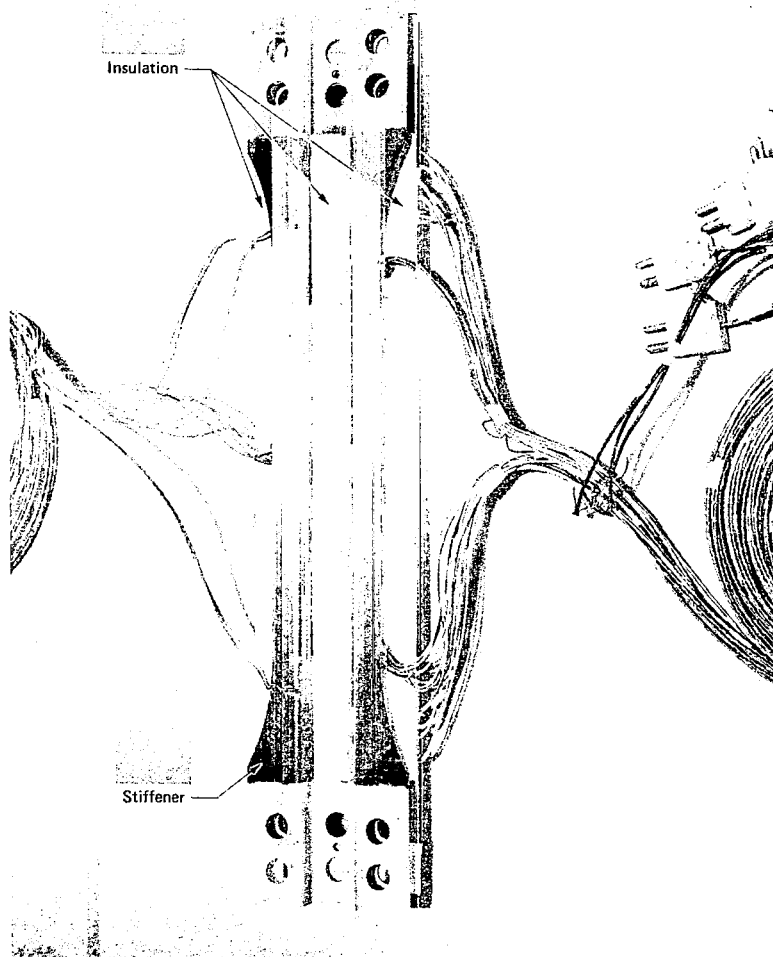Figure 23.—Thermal Analysis of Specimen for Flight-by-Flight Baseline Tests (BS-1)
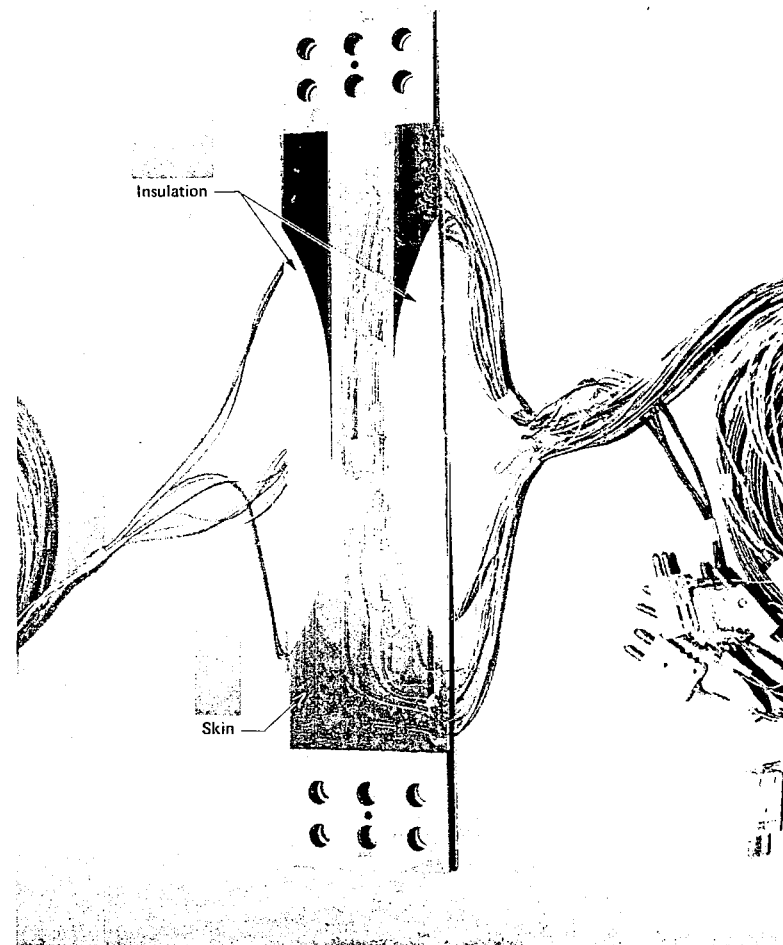
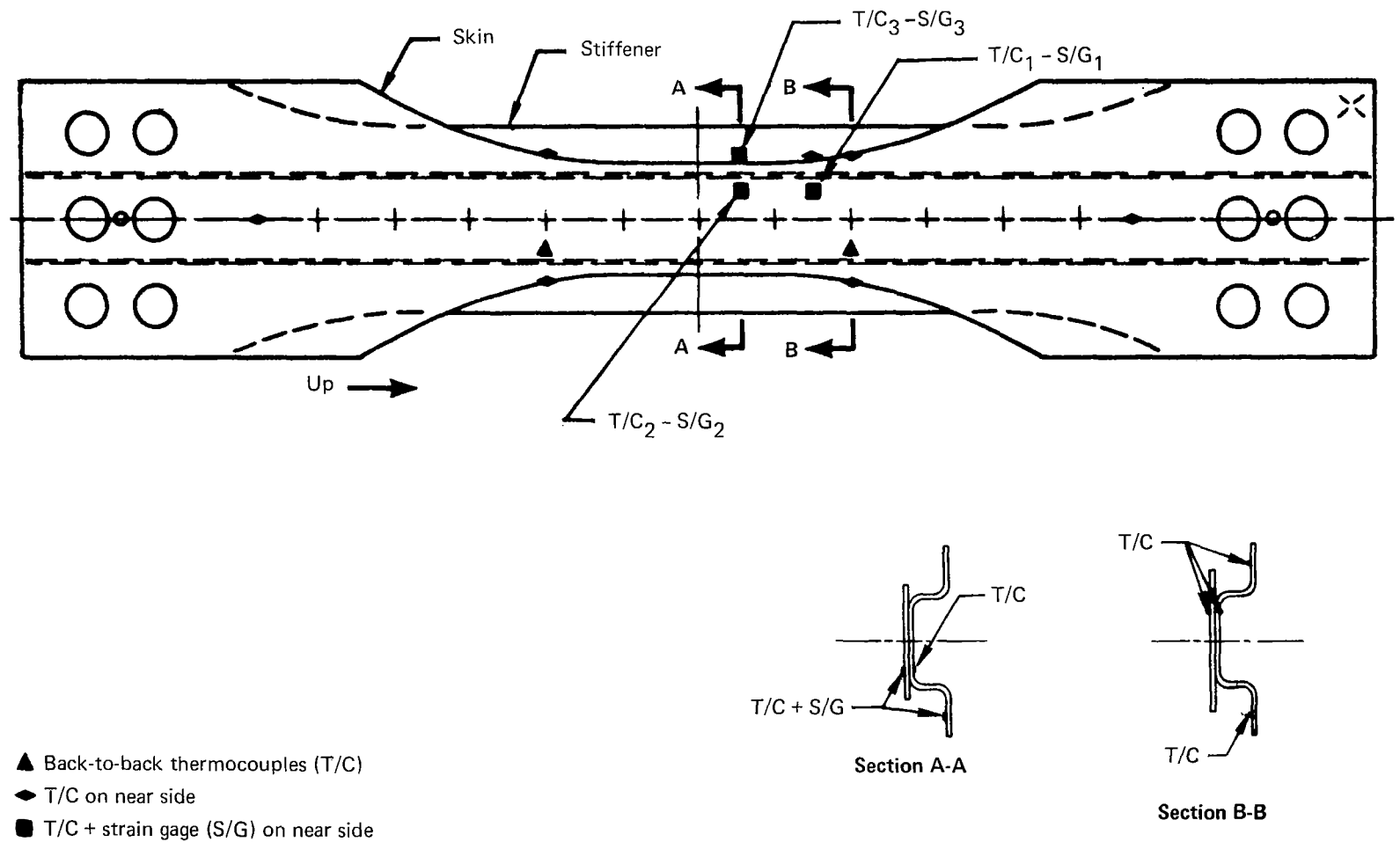*Figure 24.—BS-1 Survey Specimen Showing Insulation Details*

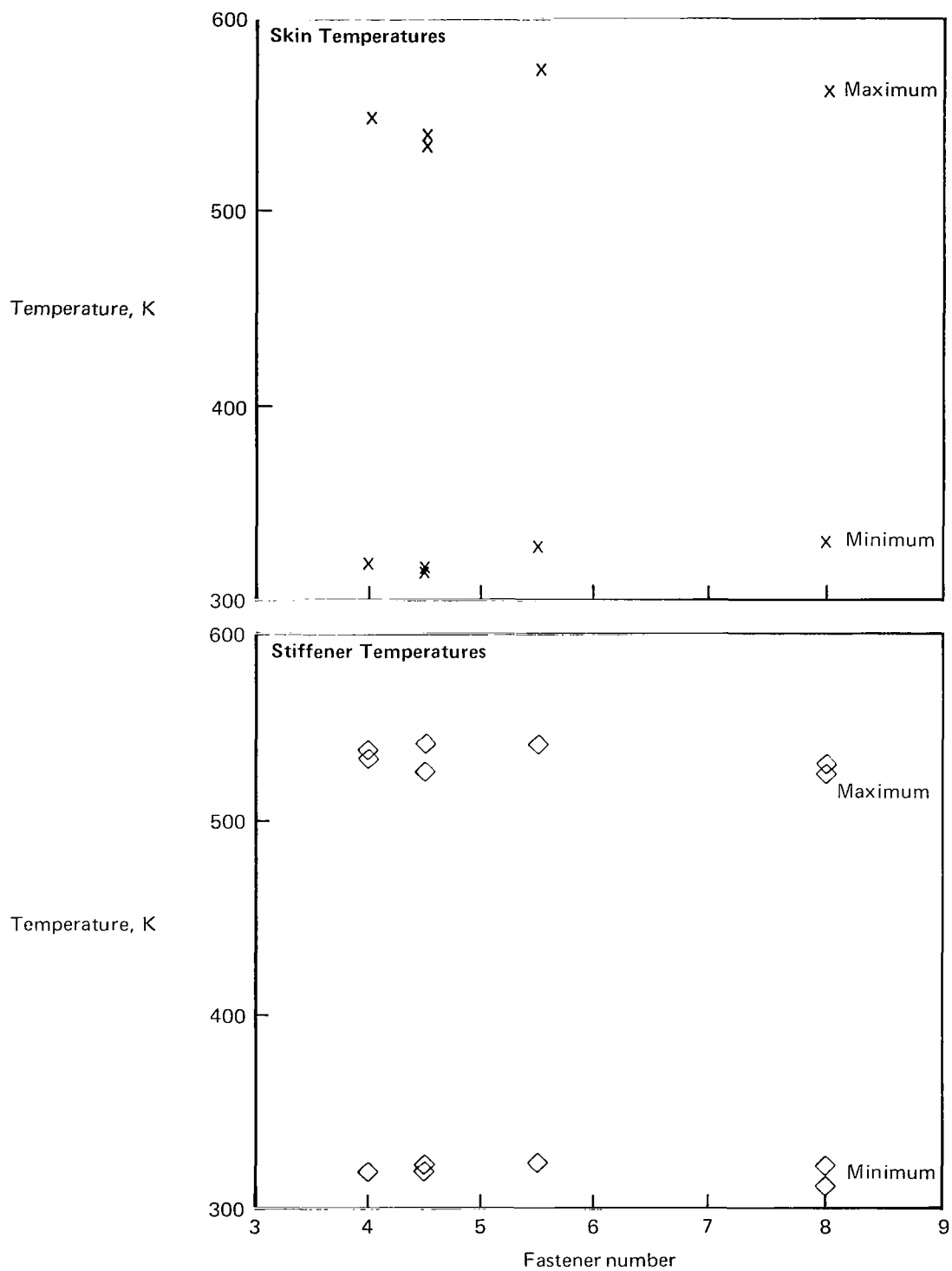Figure 25.—Instrumentation Locations for Temperature and Stress Survey (BS-1)

Figure 26.—Longitudinal Temperature Distribution, BS-1 Survey (Run 6)